nature synthesis

Article

https://doi.org/10.1038/s44160-023-00477-2

Enzymatic synthesis of organoselenium compounds via C–Se bond formation mediated by sulfur carrier proteins

Received: 2 August 2023

Accepted: 15 December 2023

Published online: 26 January 2024

Check for updates

Xingwang Zhang[1], Fangyuan Cheng[1], Jiawei Guo[1], Shanmin Zheng[1], Xuan Wang[1] & Shengying Li[1,2]

Organoselenium compounds are rare in nature but play important physiological roles by exploiting the distinct features of selenium. However, the ability to explore these compounds and their implications has been hindered by the limited availability of (bio)synthetic tools for the generation of organoselenium molecules, particularly the lack of enzymatic strategies for C–Se bond formation. Here we develop an enzymatic approach for C–Se bond formation using sulfur carrier proteins to biosynthesize the isologous selenium counterparts of cysteine, thiamine and a chuangxinmycin derivative. Our results indicate that widespread sulfur-carrier-protein-based biosynthetic systems provide promiscuous and programmable machinery for the production of unnatural Se-containing compounds. We anticipate that the 'element engineering' strategy used in this study will provide new opportunities to develop biologically rare molecules or abiological-element-containing chemicals not found in nature.

Selenium (Se) is a chalcogen element with similar chemical and physical properties to sulfur (S) and tellurium (Te)[1,2]. However, compared with S and Te, Se is kinetically labile but thermodynamically stable in the formation of organic molecules[3,4]. Due to this feature, Se-containing compounds are more reactive than their sulfur isologues but more stable than their tellurium counterparts. As a result, Se is used in nature as a trace nutrient element in several essential physiological processes by forming selenoproteins or organoselenium small molecules[5,6]. Intriguingly, organoselenium small molecules, including selenocysteine, selenomethionine, 5-methylaminomethyl-2-selenouridine and selenoneine (Fig. 1a), show chemical properties and biological functions distinct from their sulfur counterparts[1,6,7].

Inspired by nature, researchers have chemically incorporated selenium into several pharmaceutical candidates, and the products show promising abilities to adjust redox activity, improve biological uptake, fine-tune molecular conformation, enhance potency and efficacy, and antagonize drug resistance[8–12]. Thus, organoselenium compounds have emerged as potential therapeutic agents for treating a variety of diseases[12]. For example, the selenium-containing drug candidate ebselen shows strong inhibitory activity against the main protease M^{pro} of severe acute respiratory syndrome coronavirus 2 (SARS-CoV-2)[13,14]. However, studies on Se-containing drugs and bioactive small molecules remain in their infancy, mainly due to the lack of adequate (bio)synthetic tools.

Naturally occurring organoselenium products (Fig. 1a) are mostly biosynthesized via specific selenium incorporation pathways[15–18]. In synthetic chemistry, transition-metal-catalysed C–Se bond formation is a commonly used strategy to produce organoselenium compounds[19–21]. However, the lack of chemo-, regio- and/or stereoselectivity of these catalysts largely limits their applications in the complex and chiral synthesis of organoselenium molecules. In principle, sulfur-containing natural product biosynthetic enzymes may be potential biocatalysts for production of organoselenium compounds. However, due to the thermodynamic and/or kinetic discrimination of enzymes, as well as the low abundance of selenium sources, Se-containing natural products and Se-incorporating enzymatic machineries are uncommon in nature. Further, using the natural sulfur metabolic system for in vitro enzymatic incorporation of selenium is rarely successful[22–25].

[1]State Key Laboratory of Microbial Technology, Shandong University, Qingdao, China. [2]Laboratory for Marine Biology and Biotechnology, Qingdao National Laboratory for Marine Science and Technology, Qingdao, China. e-mail: lishengying@sdu.edu.cn

https://doi.org/10.1038/s44160-023-00477-2

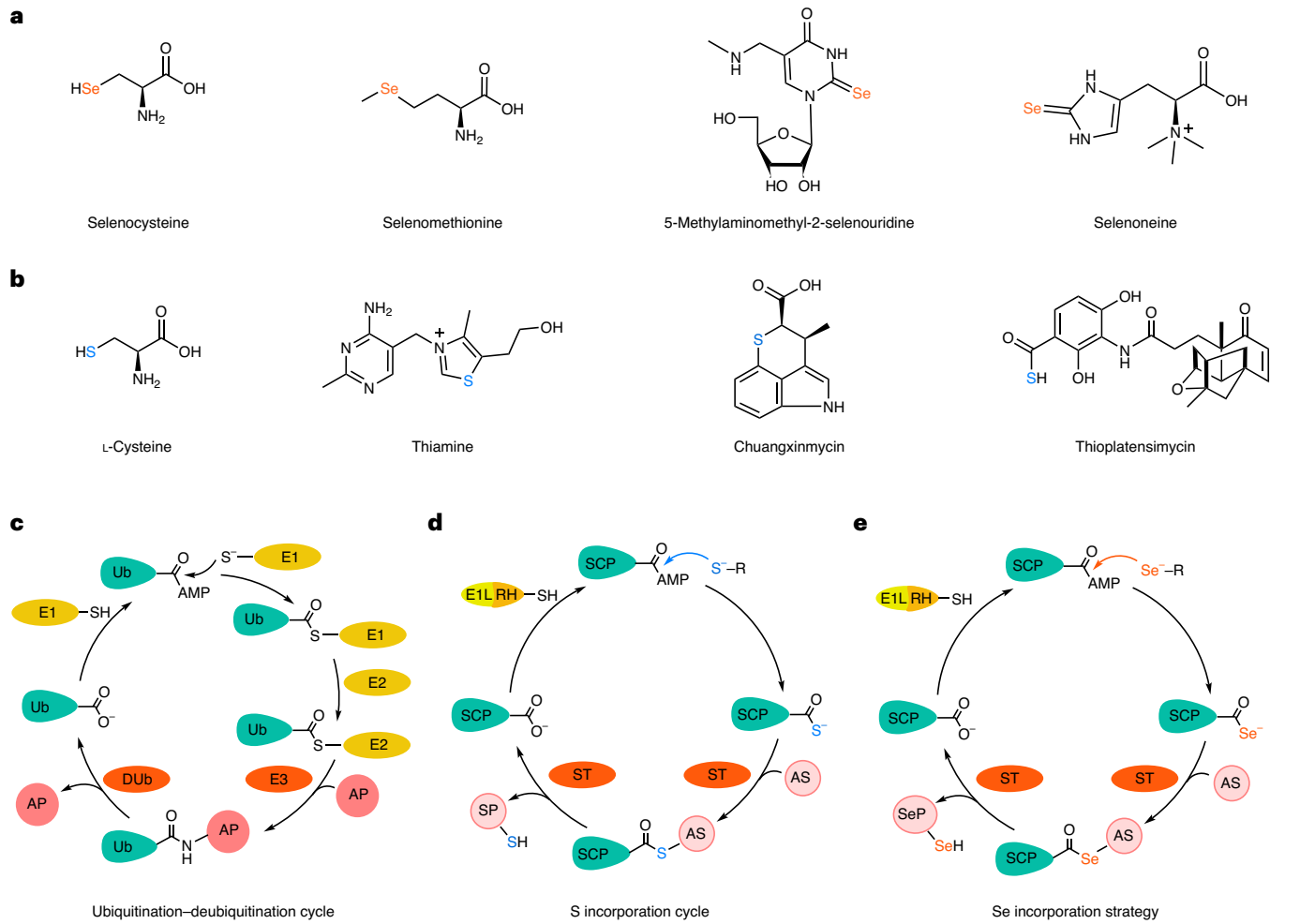

Fig. 1 | Representative selenium- and sulfur-containing natural products and the SCP-based selenium incorporation system inspired by nature. **a**, Representative selenium-containing natural products. **b**, Representative sulfur-containing natural products biosynthesized by SCP-involved pathways. **c**, The ubiquitination–deubiquitination system. During the ubiquitination–deubiquitination cycle, ubiquitin activating enzyme (E1) first forms a thioester complex with ubiquitin (Ub) via an adenylation intermediate. Then, the Ub conjugating enzyme (E2) mediates a transthioesterification reaction to produce the Ub–E2 complex, of which the Ub moiety is connected with the acceptor protein (AP) by the catalysis of Ub ligase (E3). The Ub–AP complex can be recognized either by proteasome to undergo protein degradation or by deubiquitinase (DUb) to recycle Ub. **d**, Classical SCP-based sulfur incorporation cycle. The SCP is first activated to the thiocarboxylate state by an E1-like (E1L)-activating enzyme or a fused E1L-rhodanese homologue dual-domain protein (E1L-RH) via an adenylation intermediate. Then a sulfurtransferase (ST) catalyses the connection of SCP with the acceptor substrate (AS) via a thioester bond, which is further hydrolysed to produce the sulfuration product (SP) and regenerate SCP. Different sulfur donors (HS^- or E1L–RH–$S-S^-$, indicated by $R-S^-$) can be utilized to sulfurate SCPs. **e**, The SCP-based selenium incorporation strategy developed in this study (SeP: selenylation product). Different selenium donors (HSe^- or E1L–RH–$S-Se^-$, indicated by $R-Se^-$) can be used to selenylate SCPs.

Among the large variety of sulfur-containing natural products, a small group of organosulfur compounds (Fig. 1b and Extended Data Fig. 1) are biosynthesized by employing a class of ubiquitin-like small sulfur carrier proteins (SCPs; Fig. 1b–d)[26–31]. During sulfur incorporation, SCP acts as the direct sulfur donor after its conserved C-terminal diglycine ($GG-COO^-$) motif is activated to the $GG-COS^-$ form by an E1-like (E1L) activating enzyme or a fused E1L-rhodanese homologue (RH) dual-domain protein (Fig. 1d). Subsequently, a sulfurtransferase catalyses sulfur transfer from the activated $SCP-COS^-$ to the acceptor substrate (AS), resulting in the formation of sulfur-containing products (Fig. 1d)[32]. Mechanistically, the activating enzyme and sulfurtransferase mediate two consecutive rounds of nucleophilic addition-based C–S bond formation, serving as the chemical basis for the process by which sulfur is incorporated (Fig. 1d)[28,32–34].

Se is larger than S, with an atomic radius of 1.15 Å compared to 1.00 Å for the S atom[8]. This difference leads to more loosely bound outer valence electrons and higher polarizability; as a result, Se^{2-} species such as $R-Se^-$, HSe^-, $SeSO_3^{2-}$ and $R-COSe^-$ are better nucleophiles than their S^{2-} counterparts[1,6,8]. Thus, when fed an appropriate selenium donor, the SCP-based system could show the catalytic potential needed to forge C–Se bonds and produce organoselenium compounds (Fig. 1e). To test this hypothesis based on S and Se chemistry and the biocatalytic mechanism of SCP systems, we report the SCP-based selenium replacement of the sulfur atom in three representative sulfur-containing molecules, leading to their isologous selenium counterparts, including the primary metabolites cysteine, thiamine and a secondary metabolite chuangxinmycin derivative. Our proof-of-concept exploration clearly demonstrates that SCP-based enzyme cascades can be switched to carry and transfer selenium, providing an enzymatic toolbox for producing organoselenium molecules (Fig. 1e).

Results and discussion

Protein preparation

To reconstitute the biosynthetic pathways of cysteine, thiamine and chuangxinmycin in vitro, we respectively cloned their complete biosynthetic genes from *Streptomyces coelicolor* A(3)2, *Bacillus subtilis*

https://doi.org/10.1038/s44160-023-00477-2

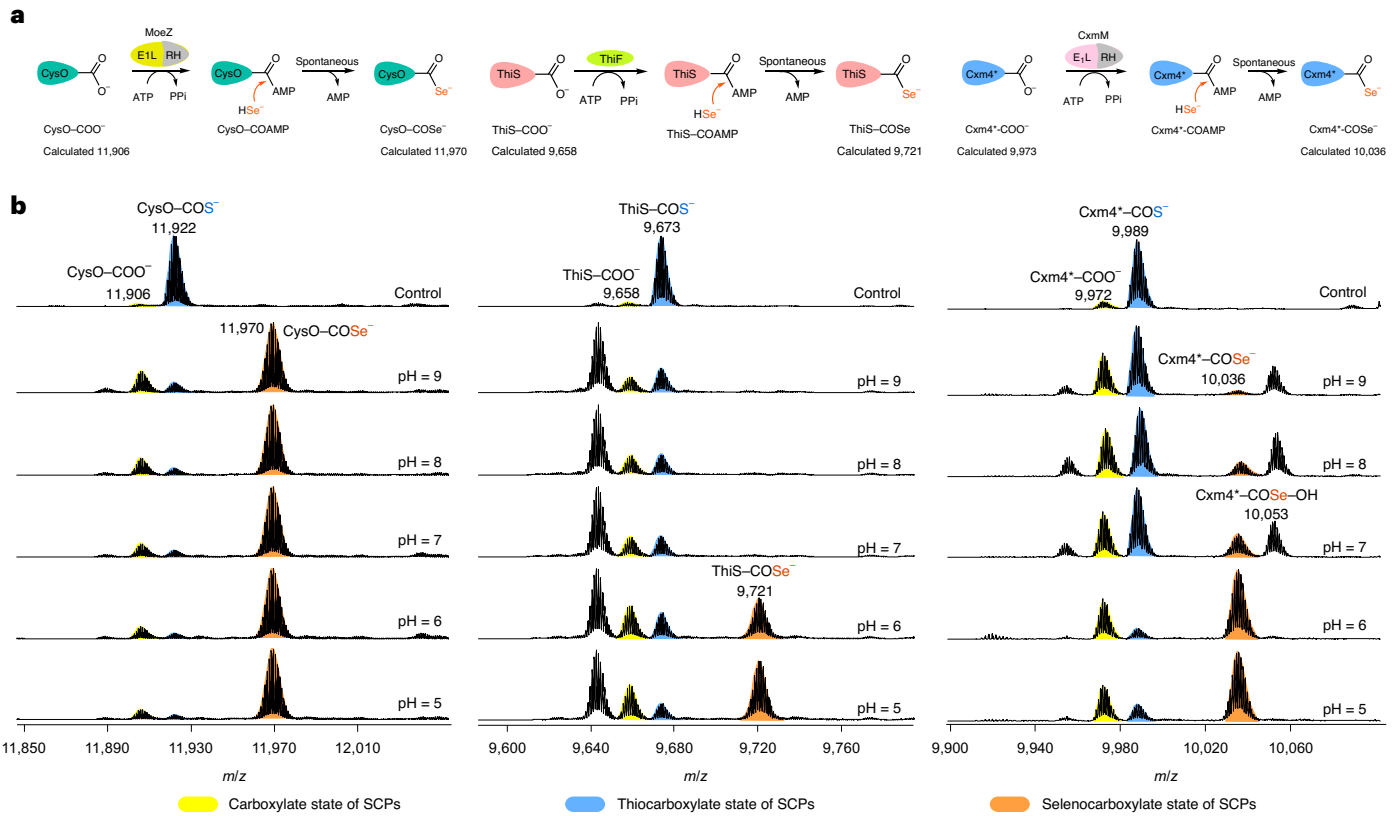

Fig. 2 | Selenylation of the SCPs. a, Schematic of ATP-dependent selenylation of CysO, ThiS and Cxm4* by MoeZ, ThiF and CxmM, respectively, using NaSeH as the selenium source. Cxm4* represents the mature form of Cxm4, of which the ten C-terminal amino acids were removed to expose the diglycine tail, and the cysteine[38] residue was mutated to alanine to prevent protein dimerization. **b**, Deconvoluted HRESI-MS analysis of the selenylation efficiency of CysO, ThiS and Cxm4* in 1 h reactions at 30 °C, under various pH conditions. The corresponding sulfuration reactions at pH 7 were used as positive controls. Note: the sulfurated SCPs observed in the selenylation reactions originated from residual sulfur species in the selenium sample, even though the commercial selenium powder used was labelled as highly pure (99.9%). E1L-RH, a fused E1-like-rhodanese homologue dual-domain protein; AMP, adenosine monophosphate; COAMP, the adenylated carboxyl group in the diglycine tail of SCPs.

and *Actinoplanes tsinanensis*. These genes were individually expressed in *Escherichia coli* BL21(DE3) or Rosetta(DE3) with suitable tags (see Supplementary Information for details). Using Ni-NTA affinity chromatography and appropriate protease treatment, all necessary proteins were purified to homogeneity (Supplementary Fig. 1).

Selenylation of the SCPs

During the SCP-mediated sulfur incorporation, an activating enzyme (that is, MoeZ for cysteine, ThiF for thiamine and CxmM for chuangxinmycin) first loads the sulfur atom onto the GG tail of SCP to generate the active thiocarboxylate species SCP–COS$^-$ (Extended Data Figs. 2–4). To investigate the selenium tolerance of the SCP-based sulfur-transfer system, we first used sodium hydroselenide (NaSeH) as a selenium donor to test the selenylation of SCPs. NaSeH was prepared by reducing selenium powder (Se^0) with sodium borohydride ($NaBH_4$) under anaerobic conditions (Supplementary Scheme 1)[35]. Then the three SCPs (CysO for cysteine, ThiS for thiamine and Cxm4* for chuangxinmycin) were individually co-incubated with their corresponding activating enzymes (Fig. 2) in the presence of adenosine triphosphate (ATP), $MgCl_2$ and freshly prepared NaSeH under neutral conditions (pH = 7) for 60 min. Of note, the reducing agent dithiothreitol (DTT) was added to keep a reducing environment for preventing the formation of diselenide. With NaSH as the sulfur source, the SCP-sulfuration reactions were performed in parallel as positive controls. The reaction mixtures were analysed by high-resolution electrospray-ionization mass spectrometry (HRESI-MS) after high-speed centrifugation was performed to remove the precipitated selenium powder. As a result, the expected selenylated CysO–COSe$^-$ and Cxm4*–COSe$^-$ were detected with conversion ratios of 87% and 17%, respectively, while ThiS–COSe$^-$ was not observed under these reaction conditions (Fig. 2b). In addition, an extra peak 17 daltons larger than the calculated mass of Cxm4*–COSe$^-$ was observed in the Cxm4* selenylation reaction, which was deduced to be the oxidation product Cxm4*–COSe–OH (Fig. 2b).

Because hydroselenides have much lower acid dissociation constant (pK_a) values than their sulfur counterparts and exhibit different pH dependences[1,36], we repeated the SCP selenylation reactions under a range of pH conditions from 5 to 9. As expected, all three SCPs were selenylated in a pH-dependent manner, with a preference for acidic conditions (Fig. 2b). Specifically, CysO–COO$^-$ was mostly converted into CysO–COSe$^-$ in all tested pH conditions at conversion ratios >80%; the highest conversion ratio reached 90% at pH 5. ThiS–COSe$^-$ was barely detected under neutral and alkaline conditions, and the highest conversion ratio was approximately 55% at pH 5. The selenylation efficiency of Cxm4* was notably affected by pH, with selenylation rates ranging from 5 to 55% when the pH was decreased from 9 to 5. In addition, lower pH conditions (pH = 5–6) inhibited the formation of the deduced byproduct Cxm4*–COSe–OH. Interestingly, when NaSH was used as a sulfur source, the SCP-sulfuration efficiency showed a reversed pH dependency (Extended Data Fig. 5). These results demonstrated SCPs could act as selenium carrier proteins when NaSeH was used as a selenium source, preferably under acidic conditions.

We attempted to use sodium selenosulfate (Na_2SeSO_3) and/or selenocysteine (Se–Cys) as alternative selenium donors to selenylate CysO (using Na_2SeSO_3), ThiS (using Se–Cys) and Cxm4* (using both

Na_2SeSO_3 and Se–Cys), as their corresponding activating enzymes were previously reported to selectively draw the S^{2-} species from the two alternative sulfur sources ($Na_2S_2O_3$ and cysteine) to sulfurate the SCPs (Extended Data Figs. 2–4)[28,30,32,37]. Of note, Na_2SeSO_3 was freshly prepared by refluxing selenium powder and Na_2SO_3 in deionized water (Supplementary Scheme 2)[38]. The pyridoxal 5′-phosphate (PLP)-dependent cysteine desulfurase IscS, which catalyses the desulfurization of cysteine to yield alanine and IscS-bound persulfide[39], was employed to hijack Se^{2-} from Se-Cys (ref. 40). Then, Na_2SeSO_3 or 'Se–Cys+IscS+PLP' were used as a selenium source to replace NaSeH in the SCP selenylation reactions (in the presence of DTT). As observed, CysO and Cxm4* were partially selenylated by Na_2SeSO_3, but with a reversed pH dependency (relative to the NaSeH systems) that favoured high-pH conditions (Supplementary Figs. 2 and 3). Cxm4* could also be selenylated by Se–Cys in a similar pH-dependent manner as NaSeH (Supplementary Fig. 3). However, the selenylation efficiencies were much lower than those observed in the corresponding NaSeH-supported reactions (Supplementary Fig. 3 and Fig. 2b). Moreover, the ThiS system could barely use Se–Cys to reach the ThiS–$COSe^-$ state (Supplementary Fig. 4).

Collectively, compared to Na_2SeSO_3 and Se–Cys, NaSeH was a better selenium source for all three SCPs. This can be fairly attributed to the different selenylation mechanisms for the three Se donors, through which the HSe^- species can spontaneously attack the adenylated carboxyl intermediates to produce the selenylated SCPs; in contrast, the Se^{2-} species in Na_2SeSO_3 and Se–Cys must be drawn and delivered to SCP with the aid of the RH domain in activating enzymes (or further cooperate with IscS and ThiI) (Extended Data Figs. 2–4). Thus, we chose NaSeH as the selenium source and pH 6 as the working condition for the following Se incorporation reactions, considering that lower pH conditions would cause more protein precipitation.

Incorporating Se into the acceptor substrates

In sulfur incorporation of cysteine, thiamine and chuangxinmycin, the sulfur atom carried by SCP–COS^- is further incorporated into the AS by a sulfurtransferase (CysM for cysteine, ThiG for thiamine and Cxm3 for chuangxinmycin) (Extended Data Figs. 2–4). After obtaining the three selenylated SCPs (CysO–$COSe^-$, ThiS–$COSe^-$ and Cxm4*–$COSe^-$), we next attempted to assemble the entire selenium incorporation pathways for the three candidate compounds (Fig. 3a–c). Experimentally, the SCP–$COSe^-$ generated in situ was co-incubated with the AS, sulfurtransferase and all necessary coenzymes and cofactors in a one-pot reaction under aerobic conditions (in the presence of DTT).

In the selenocysteine biosynthetic pathway, CysO, MoeZ, CysM and Mec^+ were co-incubated with the commercially available starting substrate O-acetyl-L-serine (OAS) and cofactors ATP, $MgCl_2$, PLP and NaSeH for 2 h at pH 6. A control reaction was performed in parallel using NaSH as a sulfur source to produce cysteine. Then, monobromobimane (mBBr), a thiol- and selenol-trapping reagent, was added to react with the expected products cysteine and Se–Cys for high-performance liquid chromatography (HPLC) analysis. As a result, the expected Cys-mBBr and Se–Cys-mBBr adducts were formed in the mBBr-treated sulfur- and selenium incorporation reactions, respectively, as evidenced by the consistent retention time and isotopic patterns with the synthetic Cys-mBBr and Se–Cys-mBBr standards (Fig. 4a and Supplementary Fig. 5). Unexpectedly, Se–Cys-mBBr was also detected in a lower yield in the control reaction with boiling-inactivated CysO (Fig. 4a). Since it was previously reported that the sulfurtransferase CysM could directly use HS^- (in addition to CysO–COS^-) as a sulfur donor to produce cysteine[26], we reasoned that CysM might also use HSe^- to generate Se–Cys.

To test this hypothesis, we first prepared purified CysO–$COSe^-$ as a selenium donor to support the reaction. Specifically, CysO–$COSe^-$ was produced by co-incubating CysO, MoeZ, ATP, $MgCl_2$ and NaSeH for 30 min. Then, the reaction mixture was buffer exchanged by gel filtration on a PD-10 column to remove the residual NaSeH. After confirming by HPLC-HRESI-MS analysis that abundant CysO–$COSe^-$ had formed in the desalted buffer (Supplementary Fig. 6), we added CysM, Mec^+, PLP and OAS to react with CysO–$COSe^-$ for another 30 min. HPLC-HRESI-MS analysis of the mBBr-treated reaction mixture clearly demonstrated the formation of Se–Cys-mBBr (Supplementary Fig. 7). Next we incubated NaSeH as the sole selenium source with CysM and OAS in the presence of PLP, $MgCl_2$ and DTT. As observed by HPLC, Se–Cys–mBBr was also formed with NaSeH concentrations ranging from 0.1 to 10 mM (Supplementary Fig. 8). Collectively, these results confirmed that CysM can use both CysO–$COSe^-$ and HSe^- as selenium sources to produce Se–Cys.

We examined whether pH conditions could influence the Se incorporation efficiency. As observed, the yield of Se–Cys-mBBr decreased notably when the pH increased from 5 to 9, clearly demonstrating the pH dependence of Se incorporation (Supplementary Fig. 9a). In contrast, the production of Cys-mBBr in the S-incorporation reaction was only slightly affected by pH (Supplementary Fig. 9b). After excluding the influence of pH on mBBr trapping efficiency against Se–Cys (Supplementary Fig. 10), we reasoned that this phenomenon was mainly due to the pH-dependent selenium transfer efficiency of CysM since the formation of CysO–$COSe^-$ was almost unaffected by pH changes (Fig. 2a and Supplementary Fig. 10). Due to the lower pK_a of R–$COSe^-$ and HSe^- (relative to their sulfur counterparts), these molecules likely become stronger nucleophiles at lower pH conditions[1,36], which is crucial for nucleophilic attack during the selenium transfer process.

According to the standard concentration curves, the yields of Se–Cys and cysteine were determined to be 9.8 ± 0.8% and 54.8 ± 1.6%, respectively, at the substrate concentration of 500 μM at pH 6 for 2 h (Supplementary Fig. 11). Taken together, the results indicate that Se–Cys can be efficiently synthesized through the SCP-based biosynthetic machinery under acidic conditions, albeit with lower efficiency than its native product cysteine. These results also revealed that a sulfurtransferase (CysM) could moonlight as a 'seleniumtransferase' by interacting with selenylated SCP (CysO–$COSe^-$) or directly using HSe^- under preferable acidic conditions. Since Se–Cys is generally biosynthesized through a specific tRNA-dependent route ($tRNA^{[Ser]Sec}$) in which tRNA-bound Se–Cys is directly recruited in the selenium-containing protein translation process[15,41,42], our finding provides an alternative method for preparation of free Se–Cys in addition to the previously developed strategy[43].

In bacteria, the biosynthesis of thiamine (as thiamine monophosphate (TMP)) includes the construction of thiazole (Thz) phosphate (Thz-P) and hydroxymethyl pyrimidine (HMP) diphosphate (HMP-PP) building blocks and condensation of these two moieties, which involves nine enzymatic reactions (Fig. 3b)[29]. To investigate the feasibility of incorporating selenium into a more complicated biosynthetic system, we attempted to produce the selenium counterpart of TMP, selenothiamine monophosphate (Se–TMP) using the SCP-based TMP biosynthetic machinery. We started by assembling the Se–Thz-P intermediate (Fig. 3b). Specifically, the in vitro reconstituted ThiS–$COSe^-$ producing kit including ThiS, ThiF, ATP, $MgCl_2$ and NaSeH was co-incubated with the chemically synthesized substrate deoxy-D-xylulose 5-phosphate (DXP), sulfurtransferase ThiG, glycine (Gly) and its oxidase ThiO, and the cofactor flavin adenine dinucleotide (FAD) for 2 h to produce Se–Thz-P1 (Fig. 3b). A natural sulfur incorporation reaction using NaSH as a sulfur donor was carried out as a positive control. Since Se–Thz-P1 and Thz-P1 are highly hydrophilic compounds and difficult to detect using HPLC, alkaline phosphatase (ALP) was added to enzymatically remove their phosphate groups at the end of the reactions (Fig. 3b). HPLC-HRESI-MS analysis showed substantial formation of Thz and Se–Thz in the S and Se–incorporation reactions, respectively (Fig. 4b). These results were confirmed by the characteristic isotope patterns of the sulfur- and selenium-containing products and comparison with the calculated exact masses (Supplementary Fig. 12). In contrast, Se–Thz

https://doi.org/10.1038/s44160-023-00477-2

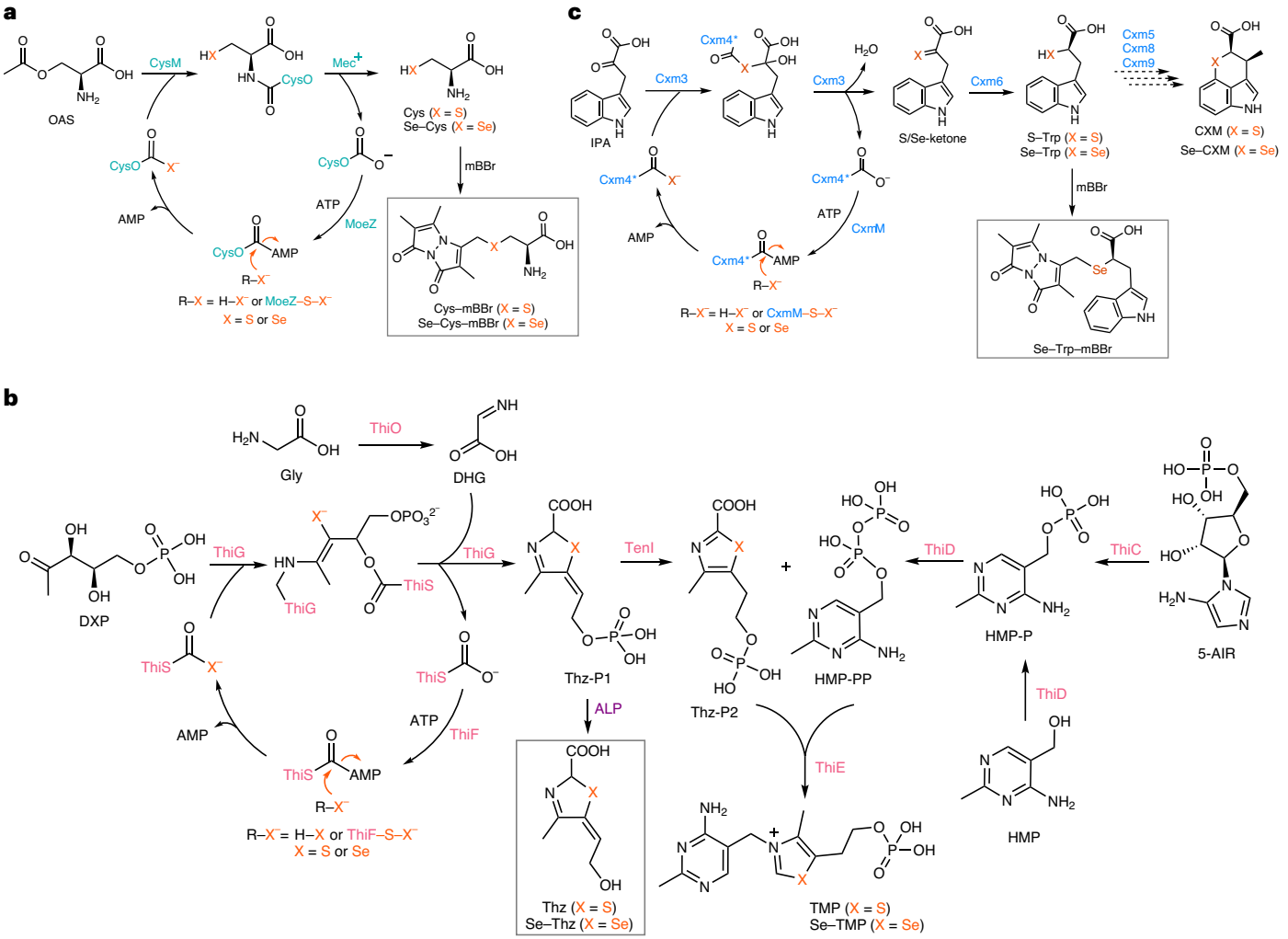

Fig. 3 | Biosynthetic pathways of the organosulfur compounds and their selenium analogues. a, Biosynthetic pathways of cysteine and Se–Cys. **b**, Biosynthetic pathways of TMP and Se–TMP. **c**, Biosynthetic pathways of S–Trp and Se–Trp. The boxed structures are mBBr-trapped or ALP-dephosphorylated derivatives used for product analysis through HPLC or HPLC-MS.

was not produced by the negative control reaction using boiled ThiS (Fig. 4b), indicating that ThiG is an SCP-specific seleniumtransferase.

Next, we attempted to assemble the entire pathway to produce Se–TMP. In the natural biosynthetic route of the HMP-PP moiety, ThiC first converts 5-aminoimidazole ribotide (5-AIR) into hydroxymethyl pyrimidine phosphate (HMP-P), which is then phosphorylated by ThiD to afford HMP-PP (Fig. 3b)[44]. As reported, ThiD can also directly transform HMP into HMP-PP via two consecutive phosphorylation steps (Fig. 3b)[45]. Thus, we used HMP as the starting material since 5-AIR is unstable and challenging to synthesize[44]. Then, HMP, ThiD, ThiE, TenI (to tautomerize Thz-P1 into Thz-P2) and KCl were further added into the Se–Thz-P1 producing system. HPLC-HRMS analysis of the two-hour reaction mixture showed the formation of Se–TMP, which was confirmed by comparing the observed isotope patterns and masses with the calculated data (Fig. 4b and Supplementary Fig. 13). Meanwhile, normal TMP was produced in the control reaction with NaSH (Fig. 4b and Supplementary Fig. 13), and no Se–TMP was formed in the negative control with heat-inactivated ThiS (Fig. 4b). Of note, we could not calculate the product yields due to the lack of authentic standards.

These results demonstrated that the complex multienzyme catalytic system can well tolerate selenium-substituted (originally sulfur-containing) substrates, intermediates and products. Thiamine is an essential cofactor that participates in several important physiological reactions—such as carbohydrate metabolism—in all living organisms and has been used to clinically treat neuritis[46]; thus, we envision that its selenium counterpart Se–TMP, which has never been found in nature nor been biosynthesized before, to our knowledge, may hold important therapeutic potential. Further research and development of Se–TMP requires much improvement of the current biosynthetic system, which is ongoing in this laboratory.

To further broaden the applicability of the SCP-based biosynthetic platform for organoselenium compounds, we attempted to incorporate Se atoms into secondary metabolites, also known as natural products, which are important for drug research and development. Chuangxinmycin (CXM) is a sulfur-containing antibiotic produced by the bacterium *A. tsinanensis* and exhibits therapeutic potential for bacterial infections due to its specific inhibitory activity against prokaryotic tryptophanyl-tRNA synthetase[47]. The biogenesis of CXM is achieved by an SCP-involving pathway (Fig. 3c)[32,48]. Therefore, we selected CXM as the target molecule for replacing its S atom with a Se atom.

In a one-pot reaction, Cxm4*, CxmM, ATP, $MgCl_2$ and NaSeH were co-incubated with the acceptor substrate indole-3-pyruvic acid (IPA), sulfurtransferase Cxm3, thioketone reductase Cxm6, nicotinamide adenine dinucleotide phosphate hydrogen (NADPH) and DTT. Subsequently, a new peak was detected by HPLC that differed from the sulfur incorporation product S–Trp, which was absent in the control reaction with boiled Cxm4* (Fig. 4c). HRESI-MS analysis indicated that

https://doi.org/10.1038/s44160-023-00477-2

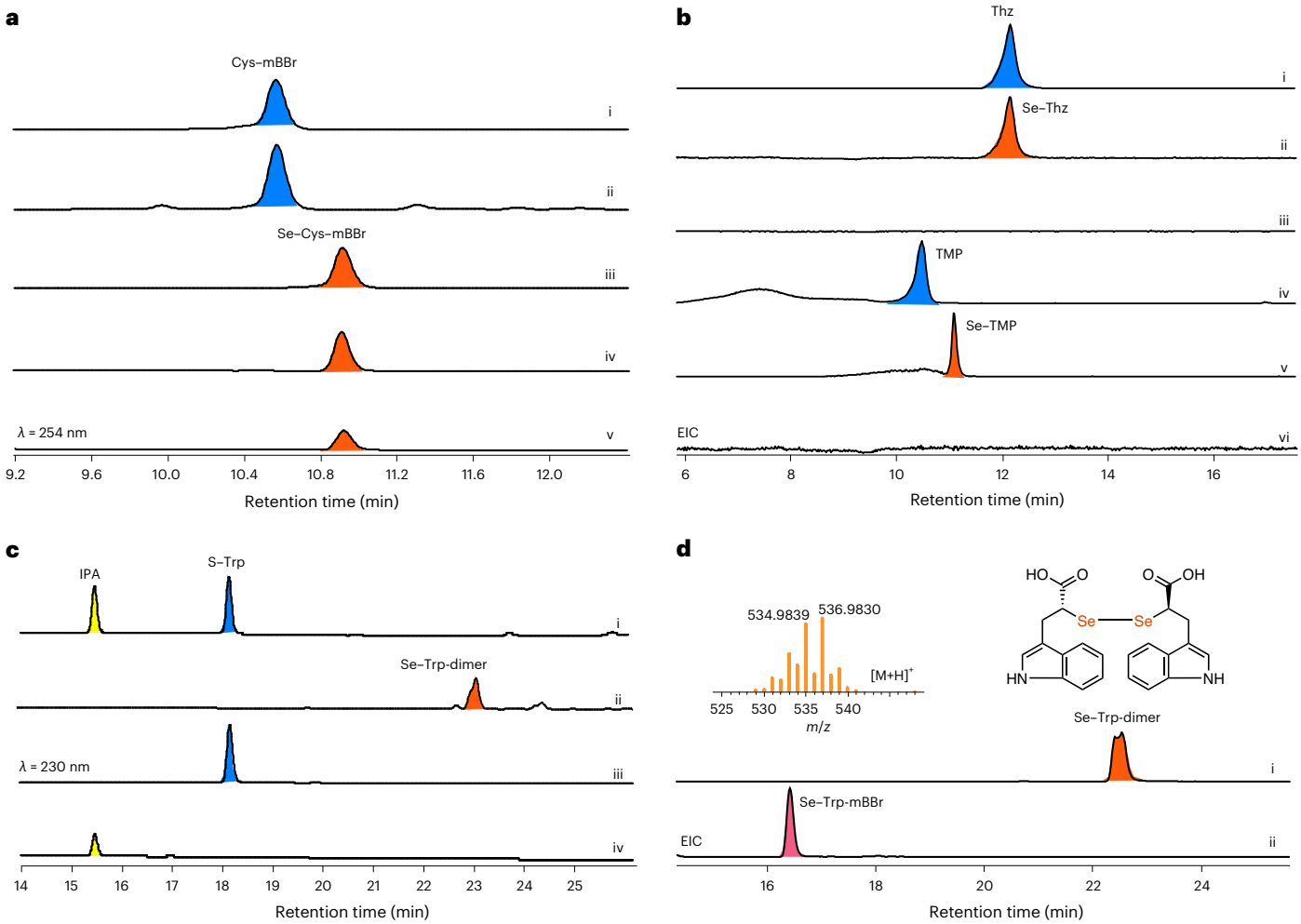

Fig. 4 | HPLC and HPLC-HRMS analyses of selenium incorporation reactions. **a**, HPLC analysis of the Se–Cys biosynthetic reactions: the Cys-mBBr standard (i); the mBBr-trapped product of the one-pot sulfur incorporation reaction (ii); the Se–Cys-mBBr standard (iii); the mBBr-trapped product of the one-pot selenium incorporation reaction (iv); and the negative control reaction with boiled CysO (v). **b**, HPLC-HRMS analysis of the biosynthetic reactions of Se–TMP: the extracted ion chromatograms (EICs) of Thz in the sulfur incorporation reaction (i) and Se–Thz in the selenium incorporation reaction (ii); the negative control reaction with boiled ThiS (iii); the EICs of TMP in the one-pot sulfur incorporation reaction (iv) and Se–TMP in the selenium incorporation reaction (v); the negative control reaction with boiled ThiS (vi). **c**, HPLC analysis of Se–Trp biosynthetic reactions: the mixed standards of IPA and S–Trp (i); the products of the Se incorporation reaction (ii) and S-incorporation reaction (iii); the negative control reaction with boiled Cxm4* (iv). **d**, HPLC-HRMS analysis of the mBBr-trapped product: the EIC of the Se–Trp-dimer before mBBr was added (i); the EIC of Se–Trp-mBBr after mBBr was added (ii). All these reactions were performed at pH 6 and 30 °C for 2 h. mBBr, monobromobimane; IPA, indole-3-pyruvic acid; S–Trp, (*R*)-3-(1H-indol-3-yl)-2-mercaptopropanoic acid; Se–Trp, (*R*)-2-hydroseleno-3-(1H-indol-3-yl)propanoic acid.

the product contained two selenium atoms, as judged by the characteristic selenium isotope pattern, implying a potential diselenide dimer (Fig. 4d and Supplementary Fig. 14). Treatment of the reaction mixture with mBBr resulted in a derivative with a single selenium atom, which exhibited a molecular weight consistent with the monomeric form of Se–Trp-mBBr (Figs. 3c and 4d; Supplementary Fig. 14). Purification of the biselenium-containing product and structure elucidation by multidimensional nuclear magnetic resonance (NMR) spectroscopy (Supplementary Figs. 15–20) confirmed that the Se incorporation product was indeed Se–Trp, but in the form of a diselenide dimer (Fig. 4d) under aerobic conditions. Interestingly, the diselenide bond could not be cleaved by generally used disulfide reducing agents, such as DTT and tris (2-carboxyethyl) phosphine, which prevented us from synthesizing Se-substituted CXM with the downstream biosynthetic enzymes (Supplementary Fig. 21). Of note, due to unavailability of Se–Trp monomer, we also could not test the activity of the downstream P450 enzyme Cxm5 towards this selenium analogue. Using the standard concentration curves of enzymatically prepared Se–Trp-dimer, the yield of Se–Trp monomer from 500 μM of substrate was determined to be 36.4 ± 1.3% comparing with 71.9 ± 1.4% of S–Trp in the sulfur incorporation reaction (Supplementary Fig. 22), at pH 6 for 2 h. These results confirmed that the Se-substituted CXM intermediate was formed, indicating that the SCP-mediated selenium incorporation system could create selenium-containing 'unnatural' natural products, which are an emerging class of compounds with therapeutic potential for a variety of diseases[12].

Enzymatic promiscuity of the Se incorporation systems

In the SCP-based sulfur- and selenium incorporation systems, the S or Se atom is sequentially transferred through protein–protein interactions between SCP–COO^- and the activating enzyme and between sulfurated or selenylated SCP and sulfurtransferase or seleniumtransferase (Fig. 1d,e). SCPs exhibit acceptor promiscuity towards activating enzymes and sulfurtransferases in different sulfur incorporation pathways. For example, during the assembly of the 2-thiosugar moiety of antibiotic BE-7585A, the activating enzyme MoeZ and sulfurtransferase BexX can co-opt SCPs from the biosynthetic pathways of cysteine and molybdopterin[30]. Similar phenomena have been observed in the biosynthesis of thioplatensimycin and chuangxinmycin[31,32]. However, the full

https://doi.org/10.1038/s44160-023-00477-2

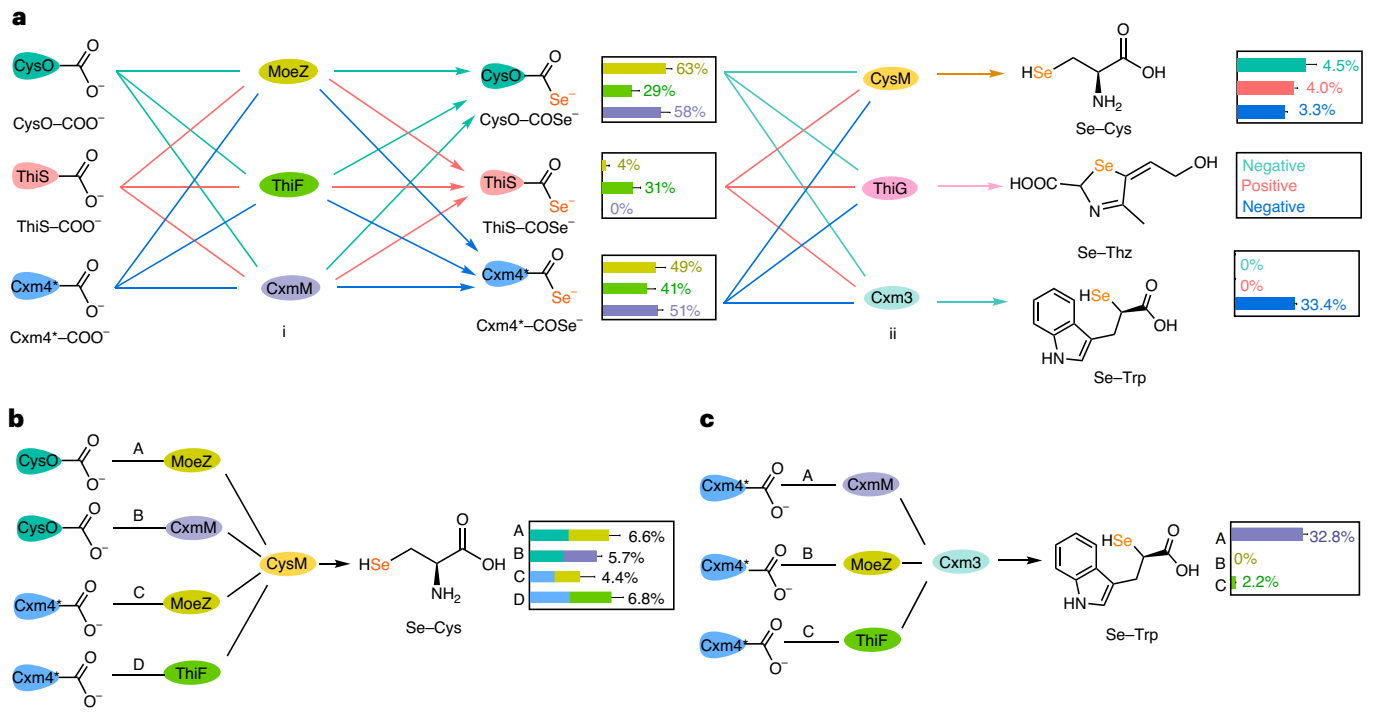

Fig. 5 | Recombination of the SCP-based selenium incorporation systems. **a**, Recombination network of SCPs for selenium incorporation with different activating enzymes MoeZ, ThiF and CxmM (i) and sulfurtransferases CysM, ThiG and Cxm3 (ii). Left: the boxed histograms show the conversion ratios of SCPs (i). Right: the boxed histograms show the yields of organoselenium products in one-pot reactions (ii) of the three recombined pathways (the yield of Se–Thz was not determined due to unavailability of authentic standard; 'Positive' indicates the product was detectable by HPLC-MS, while 'negative' means there was no detectable Se–Thz by such analysis). The colour of each column represents the corresponding same-coloured activating enzyme (in i) or SCP (in ii) supported reaction. **b**,**c**, The reprogrammed enzyme cascades for Se–Cys (**b**) and Se–Trp (**c**) biosynthesis. The boxed histograms show the product yields of the rewired routes. All these reactions were performed in triplicate at pH 6, 30 °C for 30 min. Error bars represent the standard deviations calculated from three independent experiments. Se–Cys, selenocysteine; Se–Thz, selenium-substituted thiazole derivative; Se–Trp, (*R*)-2-hydroseleno-3-(1H-indol-3-yl)propanoic acid.

landscape of promiscuous interactions between SCPs and activating enzymes and sulfurtransferases from different species has not been revealed. In particular, it is intriguing to consider whether this promiscuity could be utilized to optimize or even create unnatural selenium incorporation pathways.

First, to test the SCP selenylation efficiency of different activating enzymes, CysO, ThiS and Cxm4* were individually incubated with native and nonnative activating enzymes from the other two pathways using NaSeH as the Se source (Fig. 5a(i)). HRESI-MS analysis showed that CysO–COO⁻ could be selenylated by exogenous activating enzymes CxmM and ThiF (Fig. 5a(i)). CxmM exhibited a comparable activation ratio to the native activating enzyme MoeZ, while ThiF showed lower activity (Fig. 5a(i) and Extended Data Fig. 6a(i)). ThiS was hardly selenylated by exogenous CxmM and MoeZ, in which CxmM yielded no ThiS–COSe⁻ (Fig. 5a(i) and Extended Data Fig. 6a(ii)). Cxm4* was considerably selenylated by exogenous MoeZ and ThiF at a level comparable to that of its native partner CxmM (Fig. 5a(i) and Extended Data Fig. 6a(iii)). Control reactions using NaSH as a sulfur source showed similar reactivity patterns, although the sulfuration efficiency was higher than the corresponding selenylation efficiency (Extended Data Fig. 7a,b). These results indicate CxmM is a comparable exogenous activating enzyme for CysO, while MoeZ and ThiF are comparable exogenous activating enzymes for Cxm4* compared to their respective native activating proteins.

Next we evaluated the ability of SCP–COS⁻ and SCP–COSe⁻ to interact with different sulfurtransferases and the resulting sulfur or selenium transfer activities. We used native activating enzymes to generate SCP–COS⁻ and SCP–COSe⁻ in situ and co-incubated the product with each sulfurtransferase from different pathways, as well as related coenzymes, to generate the S- and Se-containing products (Fig. 5a(ii) and Extended Data Fig. 7a(ii)). In the sulfur-transfer reactions, CysM and ThiG could cooperate with both exogenous SCPs to accomplish the sulfur-transfer functionality, even though the yields were lower than those of their native partners; in contrast, compared to its native SCP Cxm4*, Cxm3 could only recognize CysO as an exogenous sulfur donor and produced a much lower yield of S–Trp (Extended Data Fig. 7c). In the selenium transfer reactions, the Cxm4* and ThiS participating reactions afforded comparable Se–Cys yields with those of the native CysO, while exogenous SCPs could not act as selenium donors and support selenium transfer reactions in the TMP and CXM pathways (Fig. 5a(ii) and Extended Data Fig. 6b).

After obtaining these data for enzyme promiscuity, we sought to reprogramme the SCP-based selenium incorporation processes by recombining different selenylation modules. In addition to the natural pathway CysO–MoeZ–CysM (route A), we designed the following unnatural enzymatic systems for the Se–Cys production reaction: CysO–CxmM–CysM (route B), Cxm4*–MoeZ–CysM (route C) and Cxm4*–ThiF–CysM (route D) (Fig. 5b). Three catalytic systems including Cxm4*–CxmM–Cxm3 (route A, native), Cxm4*–MoeZ–Cxm3 (route B) and Cxm4*–ThiF–Cxm3 (route C) were built for Se–Trp production (Fig. 5c). Of note, the Se–TMP biosynthetic pathway could not be reprogrammed due to the low enzyme promiscuity for SCP selenylation and selenium transfer processes (Fig. 5a). As observed, compared with the native system, all three rewired Se–Cys-producing pathways obtained comparable yields (Fig. 5b(i) and Extended Data Fig. 6c(i)). This result may be attributed to the synergistic effect of SCP–COSe⁻ and HSe⁻ towards CysM, because CysM can use both SCP–COSe⁻ and HSe⁻ as selenium donors. For the rewired Se–Trp producing processes, route C successfully produced the Se-containing product albeit in a lower yield than that of the natural system (Fig. 5c and Extended Data Fig. 6c(ii)).

Taken together, these results clearly demonstrated the promiscuity of SCPs towards activating enzymes and sulfurtransferases of exogenous origins when transferring sulfur and selenium. These promiscuities could vary a lot in different recombinations. Therefore, proper recombination of the selenylating modules can generate efficient artificial enzyme machineries to produce artificial organoselenium molecules utilizing the concept and methodology of synthetic biology.

Conclusions

Selenium and sulfur belong to the same group in the periodic table of the elements. Due to the similar physiochemical properties of these two elements, seleno-counterparts of organosulfur compounds can be developed by employing sulfur-metabolizing enzymes. In this study, we have shown that SCP-based sulfur incorporation systems can be harnessed to generate organoselenium products by functionally converting an SCP into an SeCP under appropriate reaction conditions. The carrier protein plays a crucial role in the formation of the C–Se bond through nucleophilic addition by providing essential activity-enabling and specificity-determining protein–protein interactions. Biocatalytic selenylation systems provide potential access to pharmaceutically emerging molecular architectures that are rare in nature and expand the chemoenzymatic space for organoselenium compounds. Additionally, this strategy exhibits high atomic economy by using Se^0 as the original source of selenium. Due to the promiscuities of SeCPs towards activating enzymes and seleniumtransferases, artificial enzyme machineries can be created for the production of organoselenium compounds.

SCPs, which exhibit intriguing similarity to ubiquitin in terms of structure, biochemistry and mode of action, are widely distributed in prokaryotes, eukaryotes and archaea and have roles in diverse biological functions far beyond biosynthesis[49–51]. Hence, SCP-based systems not only hold potential as a programmable biosynthetic toolbox for production of organoselenium molecules, but also provide a large enzyme pool through which the underlying physiological functions of selenium can be explored. Finally, we anticipate that the application of the 'element engineering' approach, as demonstrated in this study, will accelerate the development of unnatural chemicals that contain elements rarely or not found in biological organisms.

Methods

Chemical synthesis of NaSeH, Na_2SeSO_3, Se–Cys-mBBr, Cys-mBBr and DXP

Syntheses of NaSeH (ref. 35), Na_2SeSO_3 (ref. 38) and DXP[52,53] were carried out according to previously established methods. See Supplementary Information for synthetic schemes and NMR spectroscopy characterization details.

In vitro SCP selenylation reactions

All the bioassays in this study were repeated and measured at least three independent times. In this part, all enzymatic assays were carried out in a total volume of 50 µl in the reaction buffer (50 mM NaH_2PO_4, 100 mM NaCl, 2 mM DTT and 10% glycerol, with pH ranging from 5 to 9) at 30 °C for 60 min. The CysO selenylation reaction contained 40 µM CysO, 10 µM MoeZ, 3 mM ATP, 5 mM $MgCl_2$ and 1.5 mM newly prepared NaSeH. The ThiS selenylation reaction contained 40 µM ThiS, 10 µM ThiF, 3 mM ATP, 5 mM $MgCl_2$ and 1 mM fresh NaSeH. The Cxm4* selenylation reaction contained 40 µM Cxm4*, 10 µM CxmM, 3 mM ATP, 5 mM $MgCl_2$ and 1.5 mM freshly prepared NaSeH. For the reactions using Na_2SeSO_3 as selenium source, NaSeH was replaced with the newly prepared Na_2SeSO_3 in the same reaction conditions. For the reactions using Se–Cys as selenium source, NaSeH was replaced with the mixture of 3 mM Se–Cys, 1 µM IscS and 5 mM DTT (to reduce the oxidized Se–Cys diselenide dimer) in the same reaction conditions. As positive control reactions, sulfuration reactions of CysO, ThiS and Cxm4* using NaSH, Na_2SeSO_3 and cysteine as sulfur source to replace NaSeH, Na_2SeSO_3 and Se–Cys, respectively, were used in the same reaction systems. The reaction mixtures were frozen with liquid-nitrogen to terminate the reaction. After thawing in an ice bath, the mixtures were centrifuged at 12,000*g* and 4 °C for 10 min to remove the precipitated selenium powder. The supernatants were then analysed by HPLC-HRESI-MS using a gradient elution programme of acetonitrile (ACN) (0.1% formic acid) in H_2O (0.1% formic acid) from 5% to 90%, with a YMC-Triart Bio C4 column at 70 °C under positive ion mode.

In vitro reconstitution of the Se–Cys biosynthetic pathway

All the following enzymatic assays were carried out in a total volume of 100 µl in reaction buffer (50 mM NaH_2PO_4, 100 mM NaCl, 2 mM DTT and 10% glycerol with pH ranging from 5 to 9) at 30 °C, unless otherwise specified. The natural biosynthetic reactions of cysteine, TMP and S–Trp were used as positive control reactions, in which NaSH was used as a sulfur source to replace NaSeH in the same reaction systems. Boiled SCP proteins were used in the negative control reactions. The one-pot reaction contained 10 µM CysO, 5 µM MoeZ, 5 µM CysM, 5 µM Mec+, 3 mM ATP, 5 mM $MgCl_2$, 1.5 mM newly prepared NaSeH, 0.5 mM PLP and 500 µM OAS. The reaction was incubated for 2 h and then centrifuged to remove the precipitated selenium powder. To detect the Se–Cys-mBBr adduct, a final concentration of 10 mM mBBr was added to the supernatant and allowed to react for another 5 min in dark. The reaction was then quenched by thoroughly mixing with 200 µl methanol to precipitate proteins. The denatured proteins were removed by high-speed centrifugation at 12,000*g* for 10 min. The supernatants were then analysed using HPLC or HPLC followed by mass spectometry (HPLC-MS) with a gradient elution programme. The HPLC programme (ACN in H_2O (0.1% TFA)) was 0–1 min, 5%; 2–25 min, 5–50%; 25–26 min, 50–100%; 26–30 min, 100%; 30–31 min, 100–5%; and 31–35 min, 5%; 1 ml min^{-1}, 254 nm.

In vitro reconstitution of the Se–TMP biosynthetic pathway

The Se–Thz intermediate biosynthesis assay contained 10 µM ThiS, 5 µM ThiF, 5 µM ThiO, 5 µM ThiG, 3 mM ATP, 5 mM $MgCl_2$, 1.5 mM newly prepared NaSeH, 1 mM Gly, 2 mM FAD and 500 µM DXP. The reaction was incubated for 2 h and then centrifuged to remove the precipitated selenium powder. To remove the phosphate group in Se–Thz-P1 for HPLC detection, a final concentration of 0.2 mg ml^{-1} commercial ALP was added into the supernatant and allowed to react for another 30 min at 38 °C. Then, the reaction was quenched by thoroughly mixing with 200 µl methanol to precipitate proteins. The denatured proteins were removed by high-speed centrifugation at 12,000*g* for 10 min. The supernatants were then analysed using HPLC or HPLC-MS with a gradient elution programme. The HPLC programme (ACN in H_2O (0.1% TFA)) was 0–1 min, 2%; 2–25 min, 2–20 %; 25–26 min, 20–100%; 26–30 min, 100%; 30–31 min, 100–2%; and 31–35 min, 2%. The one-pot Se–TMP biosynthetic system contained 10 µM ThiS, 5 µM ThiF, 5 µM ThiO, 5 µM ThiG, 5 µM ThiD, 5 µM ThiE, 5 µM TenI, 6 mM ATP, 5 mM $MgCl_2$, 5 mM KCl, 1.5 mM newly prepared NaSeH, 1 mM Gly, 2 mM FAD, 1 mM HMP and 500 µM DXP. The reaction was incubated for 2 h and then centrifuged to remove the precipitated selenium powder. The reaction was then quenched by thoroughly mixing with 200 µl methanol to precipitate proteins. The denatured proteins were removed by high-speed centrifugation at 12,000*g* for 10 min. The supernatants were analysed using HPLC-MS with a gradient elution programme. The HPLC programme (ACN (10 mM ammonium acetate) in H_2O (10 mM ammonium acetate)) was 0–1 min, 1%; 2–25 min, 1–40%; 25–26 min, 40–100%; 26–30 min, 100%; 30–31 min, 100–1%; and 31–35 min, 1%; 1 ml min^{-1}, 290 nm.

In vitro reconstitution of the Se-CXM intermediate biosynthetic pathway

The Se–CXM intermediate biosynthesis assay contained 10 µM Cxm4*, 5 µM CxmM, 5 µM Cxm3, 5 µM Cxm6, 3 mM ATP, 5 mM $MgCl_2$, 5 mM NADPH, 1.5 mM newly prepared NaSeH and 500 µM IPA. The reaction was incubated for 2 h and then centrifuged to remove the precipitated

selenium powder. To detect the Se–Cys-mBBr adduct, a final concentration of 10 mM mBBr was added into the supernatant and allowed to react for another 5 min in dark. Then, the reaction was quenched by thoroughly mixing with 200 µl methanol to precipitate proteins. The denatured proteins were removed by high-speed centrifugation at 12,000*g* for 10 min. The supernatants were analysed using HPLC or HPLC-MS with a gradient elution programme. The HPLC programme (ACN in H_2O (0.1% TFA)) was 0–1 min, 20%; 2–25 min, 20–70%; 25–26 min, 70–100%; 26–30 min, 100%; 30–31 min, 100–20%; and 31–35 min, 20%; 1 ml min^{-1}, 220 nm.

SCP-activating enzyme promiscuity assays

In this part, all enzymatic assays were carried out in a total volume of 50 µl in the reaction buffer (50 mM NaH_2PO_4, 100 mM NaCl, 2 mM DTT and 10% glycerol, pH = 6) at 30 °C for 30 min. CysO promiscuity assays contained 40 µM CysO, 10 µM MoeZ or CxmM or ThiF, 3 mM ATP, 5 mM $MgCl_2$ and 1.5 mM NaSeH or NaSH. ThiS-promiscuity assays contained 40 µM ThiS, 10 µM ThiF or CxmM or MoeZ, 3 mM ATP, 5 mM $MgCl_2$ and 1.5 mM NaSeH or NaSH. Cxm4*-promiscuity assays contained 40 µM Cxm4*, 10 µM CxmM or MoeZ or ThiF, 3 mM ATP, 5 mM $MgCl_2$ and 1.5 mM NaSeH or NaSH. The reaction mixtures were frozen with liquid-nitrogen to terminate the reaction. After thawing in an ice bath, the mixtures were centrifuged at 12,000*g* and 4 °C for 10 min to remove the precipitated selenium powder. The supernatants were analysed by HPLC-HRESI-MS.

SCP-sulfurtransferase promiscuity assays

In this part, all enzymatic assays were carried out in a total volume of 100 µl in the reaction buffer (50 mM NaH_2PO_4, 100 mM NaCl, 2 mM DTT and 10% glycerol, pH = 6) at 30 °C for 30 min. CysM–ThiS promiscuity assay contained 10 µM ThiS, 5 µM ThiF, 5 µM CysM, 5 µM Mec+, 3 mM ATP, 5 mM $MgCl_2$, 1.5 mM NaSeH or NaSH, 0.5 mM PLP and 500 µM OAS. CysM–Cxm4* promiscuity assay contained 10 µM Cxm4*, 5 µM CxmM, 5 µM CysM, 5 µM Mec+, 3 mM ATP, 5 mM $MgCl_2$, 1.5 mM NaSeH or NaSH, 0.5 mM PLP and 500 µM OAS. The natural CysM–CysO assay was used as positive control. ThiG–CysO promiscuity assay contained 10 µM CysO, 5 µM MoeZ, 5 µM ThiO, 5 µM ThiG, 3 mM ATP, 5 mM $MgCl_2$, 1.5 mM NaSeH or NaSH, 1 mM Gly, 2 mM FAD and 500 µM DXP. ThiG–Cxm4* promiscuity assay contained 10 µM Cxm4*, 5 µM CxmM, 5 µM ThiO, 5 µM ThiG, 3 mM ATP, 5 mM $MgCl_2$, 1.5 mM NaSeH or NaSH, 1 mM Gly, 2 mM FAD and 500 µM DXP. The natural ThiG–ThiS assay was used as positive control. Cxm3–CysO promiscuity assay contained 10 µM CysO, 5 µM MoeZ, 5 µM Cxm3, 5 µM Cxm6, 3 mM ATP, 5 mM $MgCl_2$, 5 mM NADPH, 1.5 mM NaSeH or NaSH and 500 µM IPA. Cxm3–ThiS promiscuity assay contained 10 µM ThiS, 5 µM ThiF, 5 µM Cxm3, 5 µM Cxm6, 3 mM ATP, 5 mM $MgCl_2$, 5 mM NADPH, 1.5 mM NaSeH or NaSH and 500 µM IPA. The natural Cxm3–Cxm4* assay was used as positive control.

Reprogramming the selenium incorporation systems

In this part, all enzymatic assays were carried out in a total volume of 100 µl in the reaction buffer (50 mM NaH_2PO_4, 100 mM NaCl, 2 mM DTT and 10% glycerol, pH = 6) at 30 °C for 30 min. The CysO+CxmM+CysM assay contained 10 µM CysO, 5 µM CxmM, 5 µM CysM, 5 µM Mec+, 3 mM ATP, 5 mM $MgCl_2$, 1.5 mM NaSeH, 0.5 mM PLP and 500 µM OAS. The Cxm4*+MoeZ+CysM assay contained 10 µM Cxm4*, 5 µM MoeZ, 5 µM CysM, 5 µM Mec+, 3 mM ATP, 5 mM $MgCl_2$, 1.5 mM NaSeH, 0.5 mM PLP and 500 µM OAS. The Cxm4*+ThiF+CysM assay contained 10 µM Cxm4*, 5 µM ThiF, 5 µM CysM, 5 µM Mec+, 3 mM ATP, 5 mM $MgCl_2$, 1.5 mM NaSeH, 0.5 mM PLP and 500 µM OAS. The Cxm4*+MoeZ+Cxm3 assay contained 10 µM Cxm4*, 5 µM MoeZ, 5 µM Cxm3, 5 µM Cxm6, 3 mM ATP, 5 mM $MgCl_2$, 5 mM NADPH, 1.5 mM NaSeH or NaSH and 500 µM IPA. The Cxm4*+ThiF+Cxm3 assay contained 10 µM Cxm4*, 5 µM ThiF, 5 µM Cxm3, 5 µM Cxm6, 3 mM ATP, 5 mM $MgCl_2$, 5 mM NADPH, 1.5 mM NaSeH or NaSH and 500 µM IPA. The corresponding native biosynthetic reactions were used as positive controls.

Reporting summary

Further information on research design is available in the Nature Portfolio Reporting Summary linked to this article.

Data availability

Experimental data supporting the conclusions of this study are available within the article and its Supplementary information. Protein sequences are retrieved from the NCBI protein database (https://www.ncbi.nlm.nih.gov/protein/) with the accession numbers in Supplementary Table 1.

References

1. Wessjohann, L. A., Schneider, A., Abbas, M. & Brandt, W. Selenium in chemistry and biochemistry in comparison to sulfur. *Biol. Chem.* **388**, 997–1006 (2007).
2. Clive, D. L. J. et al. Organic tellurium and selenium chemistry. Reduction of tellurides, delenides, and delenoacetals with triphenyltin hydride. *J. Am. Chem. Soc.* **102**, 4438–4447 (1980).
3. Mukherjee, A. J., Zade, S. S., Singh, H. B. & Sunoj, R. B. Organoselenium chemistry: role of intramolecular interactions. *Chem. Rev.* **110**, 4357–4416 (2010).
4. Chivers, T. & Laitinen, R. S. Tellurium: a maverick among the chalcogens. *Chem. Soc. Rev.* **44**, 1725–1739 (2015).
5. Weekley, C. M. & Harris, H. H. Which form is that? The importance of selenium speciation and metabolism in the prevention and treatment of disease. *Chem. Soc. Rev.* **42**, 8870–8894 (2013).
6. Reich, H. J. & Hondal, R. J. Why nature chose selenium. *ACS Chem. Biol.* **11**, 821–841 (2016).
7. Birringer, M., Pilawa, S. & Flohe, L. Trends in selenium biochemistry. *Nat. Prod. Rep.* **19**, 693–718 (2002).
8. Hou, W. & Xu, H. Incorporating selenium into heterocycles and natural products—from chemical properties to pharmacological activities. *J. Med. Chem.* **65**, 4436–4456 (2022).
9. Chuai, H. Y. et al. Small molecule selenium-containing compounds: recent development and therapeutic applications. *Eur. J. Med. Chem.* **223**, 113621–113641 (2021).
10. Raffa, R. B. Diselenium, instead of disulfide, bonded analogs of conotoxins: novel synthesis and pharmacotherapeutic potential. *Life Sci.* **87**, 451–456 (2010).
11. Tan, Y., Wang, M. & Chen, Y. Reprogramming the biosynthesis of precursor peptide to create a selenazole-containing nosiheptide analogue. *ACS Synth. Biol.* **11**, 85–91 (2022).
12. Hou, W. et al. Selenium as an emerging versatile player in heterocycles and natural products modification. *Drug Discov. Today* **27**, 2268–2277 (2022).
13. Jin, Z. M. et al. Structure of M^{pro} from SARS-CoV-2 and discovery of its inhibitors. *Nature* **582**, 289–293 (2020).
14. Amporndanai, K. et al. Inhibition mechanism of SARS-CoV-2 main protease by ebselen and its derivatives. *Nat. Commun.* **12**, 3061–3068 (2021).
15. Turanov, A. A. et al. Biosynthesis of selenocysteine, the 21st amino acid in the genetic code, and a novel pathway for cysteine biosynthesis. *Adv. Nutr.* **2**, 122–128 (2011).
16. Kayrouz, C. M., Huang, J., Hauser, N. & Seyedsayamdost, M. R. Biosynthesis of selenium-containing small molecules in diverse microorganisms. *Nature* **610**, 199–204 (2022).
17. Wittwer, A. J., Tsai, L., Ching, W. M. & Stadtman, T. C. Identification and synthesis of a naturally occurring selenonucleoside in bacterial tRNAs: 5-[(methylamino)methyl]-2-selenouridine. *Biochemistry* **23**, 4650–4655 (1984).

18. Schrauzer, G. N. Selenomethionine: a review of its nutritional significance, metabolism and toxicity. *J. Nutr.* **130**, 1653–1656 (2000).
19. Sonawane, A. D. & Koketsu, M. Recent advances on C–Se bond-forming reactions at low and room temperature. *Curr. Org. Chem.* **23**, 3206–3225 (2020).
20. Rafique, J., Canto, R. F. S., Saba, S., Barbosa, F. A. R. & Braga, A. L. Recent advances in the synthesis of biologically relevant selenium-containing 5-membered heterocycles. *Curr. Org. Chem.* **20**, 166–188 (2016).
21. Beletskaya, I. P. & Ananikov, V. P. Transition-metal-catalyzed C–S, C–Se, and C–Te bond formation via cross-coupling and atom-economic addition reactions. *Chem. Rev.* **111**, 1596–1636 (2011).
22. Reich, H. J., Yelm, K. E. & Wollowitz, S. Kinetics, thermodynamics, and stereochemistry of the allyl sulfoxide sulfenate and selenoxide selenenate [2,3] sigmatropic rearrangements. *J. Am. Chem. Soc.* **105**, 2503–2504 (1983).
23. Collins, R. et al. Biochemical discrimination between selenium and sulfur 1: a single residue provides selenium specificity to human selenocysteine lyase. *PLoS ONE* **7**, e30581 (2012).
24. Johansson, A. L., Collins, R., Arner, E. S. J., Brzezinski, P. & Hogbom, M. Biochemical discrimination between selenium and sulfur 2: mechanistic investigation of the selenium specificity of human selenocysteine lyase. *PLoS ONE* **7**, e30528 (2012).
25. Cheng, R. et al. Implications for an imidazol-2-yl carbene intermediate in the rhodanase-catalyzed C–S bond formation reaction of anaerobic ergothioneine biosynthesis. *ACS Catal.* **11**, 3319–3334 (2021).
26. O'Leary, S. E., Jurgenson, C. T., Ealick, S. E. & Begley, T. P. O-Phospho-L-serine and the thiocarboxylated sulfur carrier protein CysO-COSH are substrates for CysM, a cysteine synthase from *Mycobacterium tuberculosis*. *Biochemistry* **47**, 11606–11615 (2008).
27. Burns, K. E. et al. Reconstitution of a new cysteine biosynthetic pathway in *Mycobacterium tuberculosis*. *J. Am. Chem. Soc.* **127**, 11602–11603 (2005).
28. Dorrestein, P. C., Zhai, H. L., McLafferty, F. W. & Begley, T. P. The biosynthesis of the thiazole phosphate moiety of thiamin: the sulfur transfer mediated by the sulfur carrier protein ThiS. *Chem. Biol.* **11**, 1373–1381 (2004).
29. Jurgenson, C. T., Begley, T. P. & Ealick, S. E. The structural and biochemical foundations of thiamin biosynthesis. *Annu. Rev. Biochem.* **78**, 569–603 (2009).
30. Sasaki, E. et al. Co-opting sulphur-carrier proteins from primary metabolic pathways for 2-thiosugar biosynthesis. *Nature* **510**, 427–431 (2014).
31. Dong, L. B. et al. Biosynthesis of thiocarboxylic acid-containing natural products. *Nat. Commun.* **9**, 2362 (2018).
32. Zhang, X. et al. Biosynthesis of chuangxinmycin featuring a deubiquitinase-like sulfurtransferase. *Angew. Chem. Int. Ed.* **60**, 24418–24423 (2021).
33. Jurgenson, C. T., Burns, K. E., Begley, T. P. & Ealick, S. E. Crystal structure of a sulfur carrier protein complex found in the cysteine biosynthetic pathway of *Mycobacterium tuberculosis*. *Biochemistry* **47**, 10354–10364 (2008).
34. Sasaki, E. & Liu, H. W. Mechanistic studies of the biosynthesis of 2-thiosugar: evidence for the formation of an enzyme-bound 2-Ketohexose intermediate in BexX-catalyzed reaction. *J. Am. Chem. Soc.* **132**, 15544–15546 (2010).
35. Klayman, D. L. & Griffin, T. S. Reaction of selenium with sodium borohydride in protic solvents. A facile method for introduction of selenium into organic molecules. *J. Am. Chem. Soc.* **95**, 197–200 (1973).
36. Zhu, D. F., Zheng, W. R., Chang, H. F. & Xie, H. Y. A theoretical study on the pK_a values of selenium compounds in aqueous solution. *New J. Chem.* **44**, 8325–8336 (2020).
37. Cipollone, R., Ascenzi, P. & Visca, P. Common themes and variations in the rhodanese superfamily. *IUBMB Life* **59**, 51–59 (2007).
38. Liu, L. P., Peng, Q. & Li, Y. D. Preparation of monodisperse Se colloid spheres and Se nanowires using Na_2SeSO_3 as precursor. *Nano. Res.* **1**, 403–411 (2008).
39. Cupp-Vickery, J. R., Urbina, H. & Vickery, L. E. Crystal structure of IscS, a cysteine desulfurase from *Escherichia coli*. *J. Mol. Biol.* **330**, 1049–1059 (2003).
40. Mihara, H., Kurihara, T., Yoshimura, T., Soda, K. & Esaki, N. Cysteine sulfinate desulfinase, a NIFS-like protein of *Escherichia coli* with selenocysteine lyase and cysteine desulfurase activities. Gene cloning, purification, and characterization of a novel pyridoxal enzyme. *J. Biol. Chem.* **272**, 22417–22424 (1997).
41. Silva, I. R. et al. Formation of a ternary complex for selenocysteine biosynthesis in bacteria. *J. Biol. Chem.* **290**, 29178–29188 (2015).
42. Mueller, E. G. Se-ing into selenocysteine biosynthesis. *Nat. Chem. Biol.* **5**, 611–612 (2009).
43. Esaki, N. & Soda, K. Preparation of sulfur and selenium amino-acids with microbial pyridoxal-phosphate enzymes. *Method. Enzymol.* **143**, 291–297 (1987).
44. Lawhorn, B. G., Mehl, R. A. & Begley, T. P. Biosynthesis of the thiamin pyrimidine: the reconstitution of a remarkable rearrangement reaction. *Org. Biomol. Chem.* **2**, 2538–2546 (2004).
45. Cheng, G., Bennett, E. M., Begley, T. P. & Ealick, S. E. Crystal structure of 4-amino-5-hydroxymethyl-2-methylpyrimidine phosphate kinase from *Salmonella typhimurium* at 2.3 Å resolution. *Structure* **10**, 225–235 (2002).
46. Manzetti, S., Zhang, J. & van der Spoel, D. Thiamin function, metabolism, uptake, and transport. *Biochemistry* **53**, 821–835 (2014).
47. Xu, X. et al. Heterologous expression guides identification of the biosynthetic gene cluster of chuangxinmycin, an indole alkaloid antibiotic. *J. Nat. Prod.* **81**, 1060–1064 (2018).
48. Fan, S. et al. Structural insights into the specific interaction between *Geobacillus stearothermophilus* tryptophanyl-tRNA synthetase and antimicrobial chuangxinmycin. *J. Biol. Chem.* **298**, 101580 (2022).
49. Maupin-Furlow, J. A. Ubiquitin-like proteins and their roles in archaea. *Trends Microbiol.* **21**, 31–38 (2013).
50. Iyer, L. M., Burroughs, A. M. & Aravind, L. The prokaryotic antecedents of the ubiquitin-signaling system and the early evolution of ubiquitin-like β-grasp domains. *Genome Biol.* **7**, R60 (2006).
51. Tanabe, T. S., Leimkuhler, S. & Dahl, C. The functional diversity of the prokaryotic sulfur carrier protein TusA. *Adv. Microb. Physiol.* **75**, 233–277 (2019).
52. Taylor, S. V. et al. Chemical and enzymatic synthesis of 1-deoxy-D-xylulose-5-phosphate. *J. Org. Chem.* **63**, 2375–2377 (1998).
53. Meyer, O., Grosdemange-Billiard, C., Tritsch, D. & Rohmer, M. Synthesis and activity of two trifluorinated analogues of 1-deoxy-D-xylulose 5-phosphate. *Tetrahedron Lett.* **48**, 711–714 (2007).

Acknowledgements

We thank J. Qu, G. Lin, J. Zhu, Z. Li and H. Sui from the State Key Laboratory of Microbial Technology at Shandong University for their guidance and help in HPLC-MS and NMR spectroscopy analyses. This work was supported by National Key Research and Development Program of China (2022YFC2804500 to X.Z.), National Natural Science Foundation of China (32025001 to S.L., 22237004 to

S.L., 32000039 to X.Z.) and Shandong Provincial Natural Science Foundation (ZR2023ZD50 to X.Z., ZR2019ZD20 to S.L.).

Author contributions

S.L. designed this study and analysed the results. X.Z. synthesized the substrates, performed the bioassays and analysed the results. F.C., J.G., S.Z. and X.W. cloned the genes, constructed the protein expression vectors and purified the proteins. X.Z. and S.L. wrote and revised the paper.

Competing interests

The authors declare no competing interests.

Additional information

Supplementary information The online version contains supplementary material available at https://doi.org/10.1038/s44160-023-00477-2.

Extended data is available for this paper at https://doi.org/10.1038/s44160-023-00477-2.

Correspondence and requests for materials should be addressed to Shengying Li.

Peer review information *Nature Synthesis* thanks the anonymous reviewers for their contribution to the peer review of this work. Primary Handling Editor: Thomas West, in collaboration with the *Nature Synthesis* team.

https://doi.org/10.1038/s44160-023-00477-2

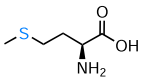
L-Methionine

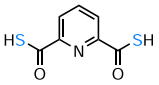
2,6-Pyridinedicarbothioic acid

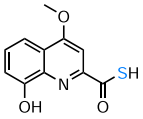
Thioquinolobactin

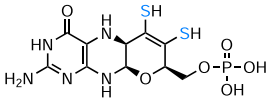
Molybdopterin

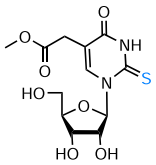
5-Methoxycarbonylmethyl-2-thiouridine

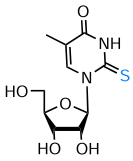
2-Thioribothymidine

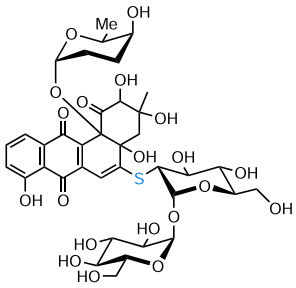
BE-7585A

Extended Data Fig. 1 | Representative sulfur-containing natural products biosynthesized by SCP-involved pathways. Additional organosulfur structures to Fig. 1.

https://doi.org/10.1038/s44160-023-00477-2

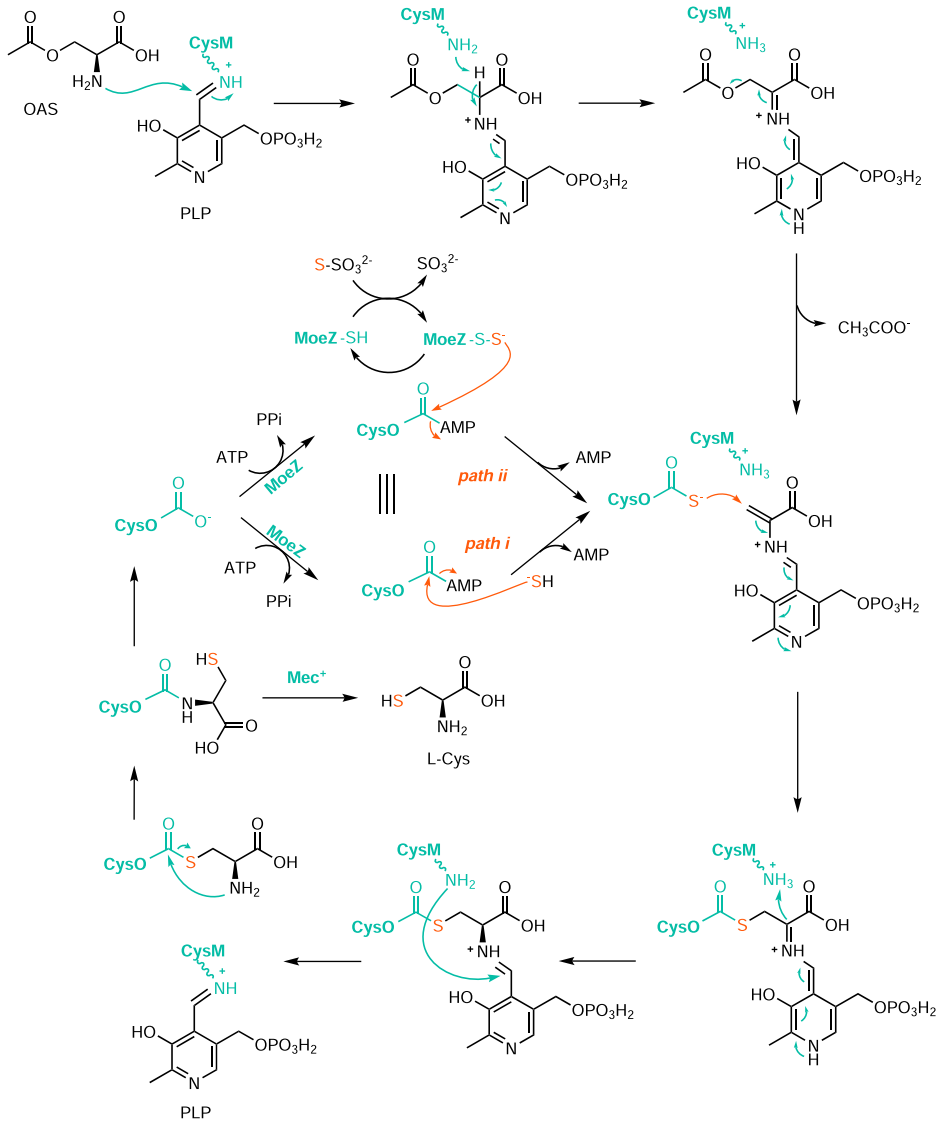

Extended Data Fig. 2 | Enzymatic mechanism of the sulfur incorporation process in cysteine biosynthesis. Key nucleophilic attack reactions are indicated by orange arrows. The sulfur source for CysO sulfuration can be either HS^- (*path i*) or $S_2O_3^{2-}$ (*path ii*).

https://doi.org/10.1038/s44160-023-00477-2

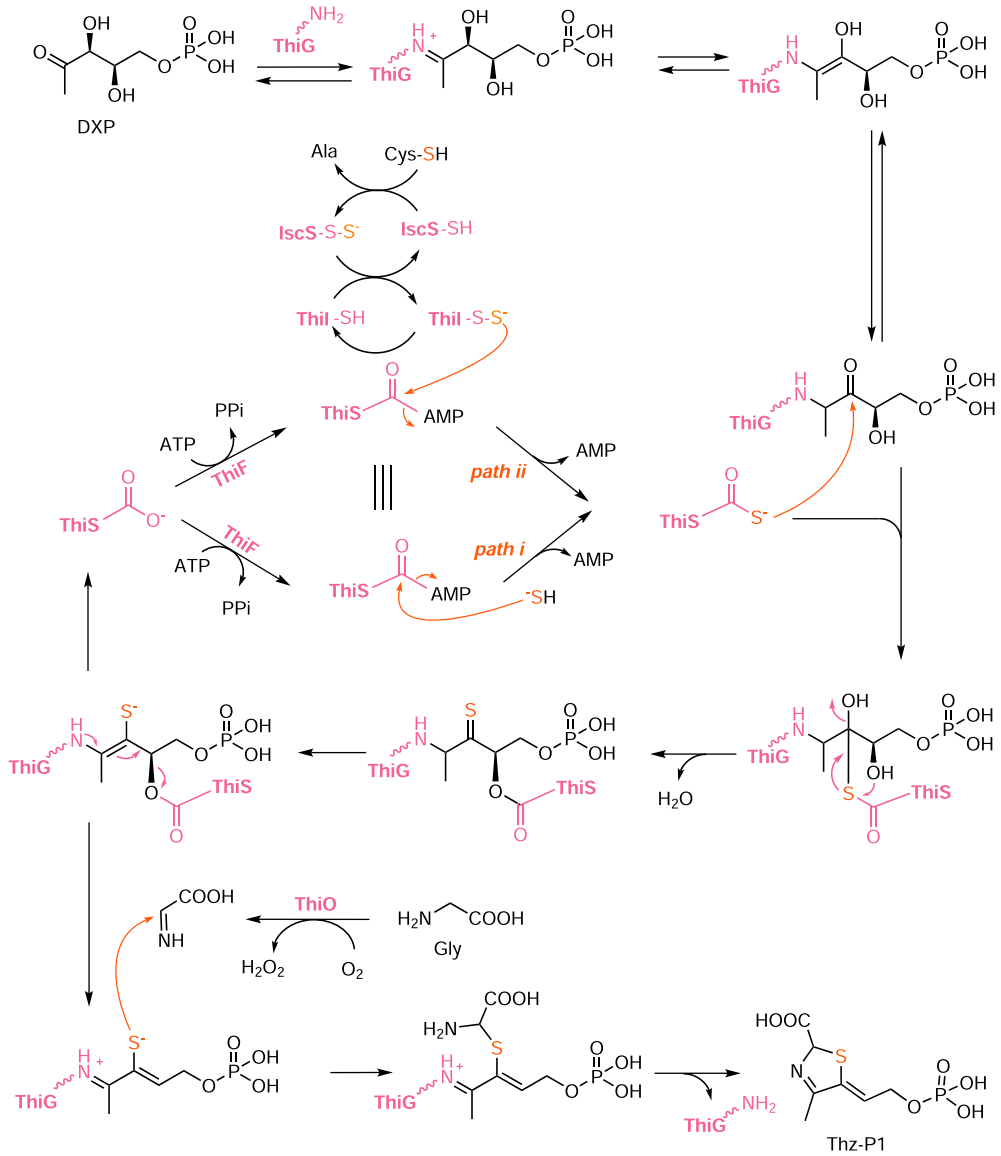

Extended Data Fig. 3 | Enzymatic mechanism of the sulfur incorporation process in thiamin biosynthesis. Key nucleophilic attack reactions are indicated by orange arrows. The sulfur source for ThiS sulfuration can be either HS^- (*path i*) or L-Cys (*path ii*).

https://doi.org/10.1038/s44160-023-00477-2

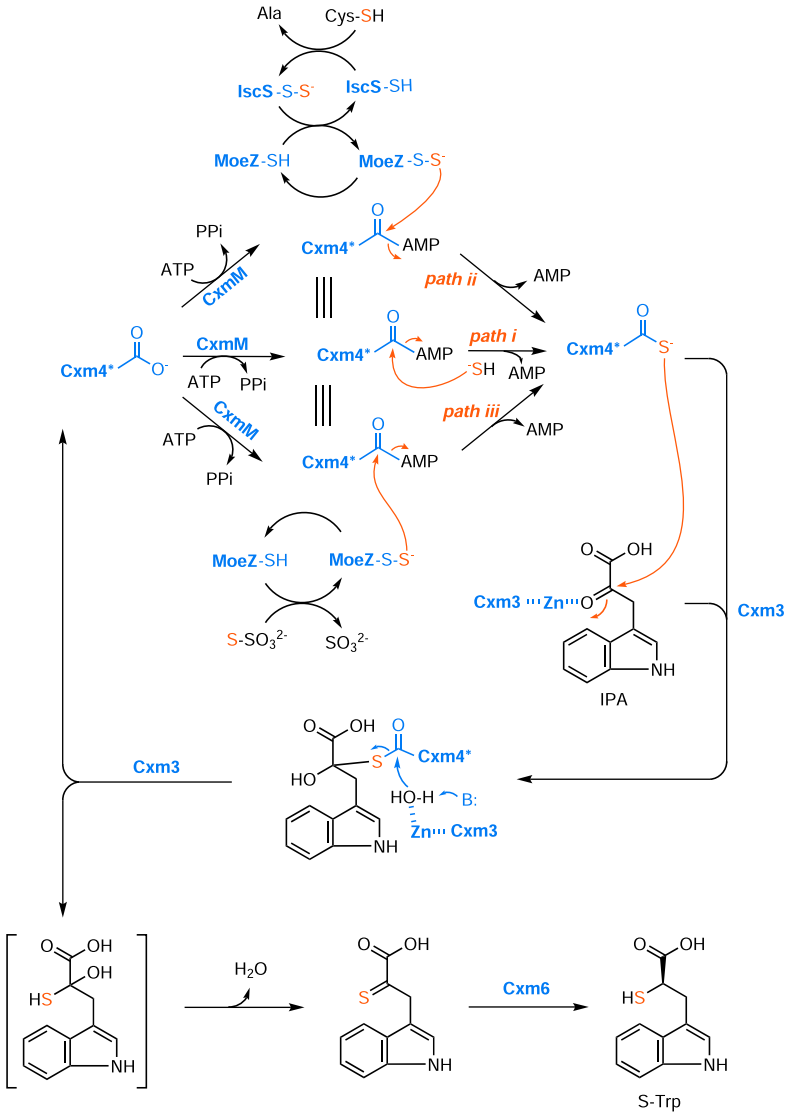

Extended Data Fig. 4 | Enzymatic mechanism of the sulfur incorporation process in chuangxinmycin biosynthesis. Key nucleophilic attack reactions are indicated by orange arrows. The sulfur source for Cxm4* sulfuration can be HS^- (*path i*), L-Cys (*path ii*) or $S_2O_3^{2-}$ (*path iii*).

https://doi.org/10.1038/s44160-023-00477-2

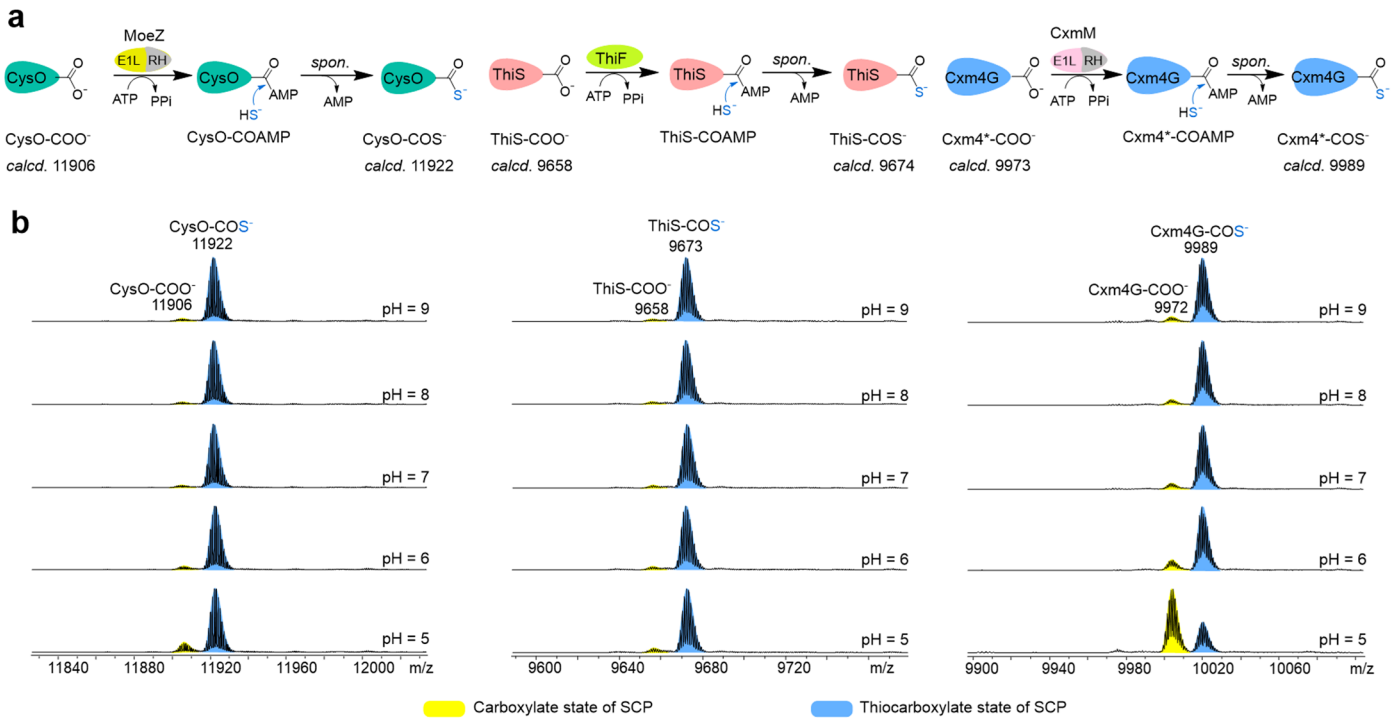

Extended Data Fig. 5 | Sulfuration of the SCPs. a, Schematic ATP-dependent sulfuration of CysO, ThiS, and Cxm4G (the matured form of Cxm4) by MoeZ, ThiF, and CxmM, respectively, with NaSH as the sulfur source. **b**, Deconvoluted HRESI-MS analysis of the sulfuration efficiency of CysO, ThiS, and Cxm4* under different pH conditions.

https://doi.org/10.1038/s44160-023-00477-2

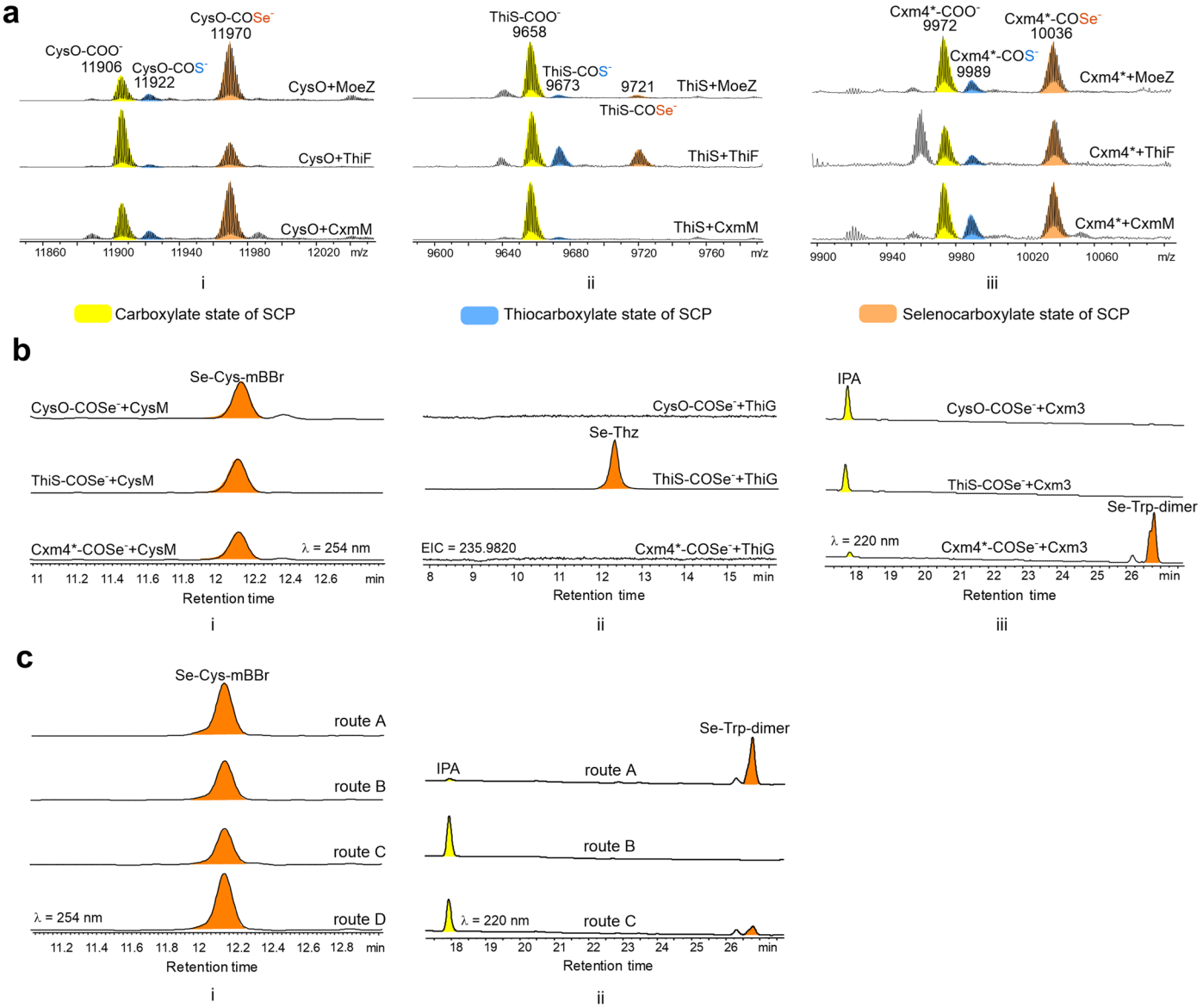

Extended Data Fig. 6 | HRESI-MS/HPLC analysis of the recombined SCP-based selenium incorporation systems. a, Deconvoluted HRESI-MS analyses of the selenylation efficiency of CysO (i), ThiS (ii) and Cxm4* (iii) by different activating enzymes. **b**, HPLC (i and iii) and HPLC-MS (ii) analysis of Se-Cys (i), Se-Thz (ii), and Se-Trp (iii) using different selenylated SCPs (that is, SCP-COSe⁻) as selenium donors. **c**, HPLC analysis of Se-Cys (i) and Se-Trp (ii) produced in the reprogrammed pathways.

https://doi.org/10.1038/s44160-023-00477-2

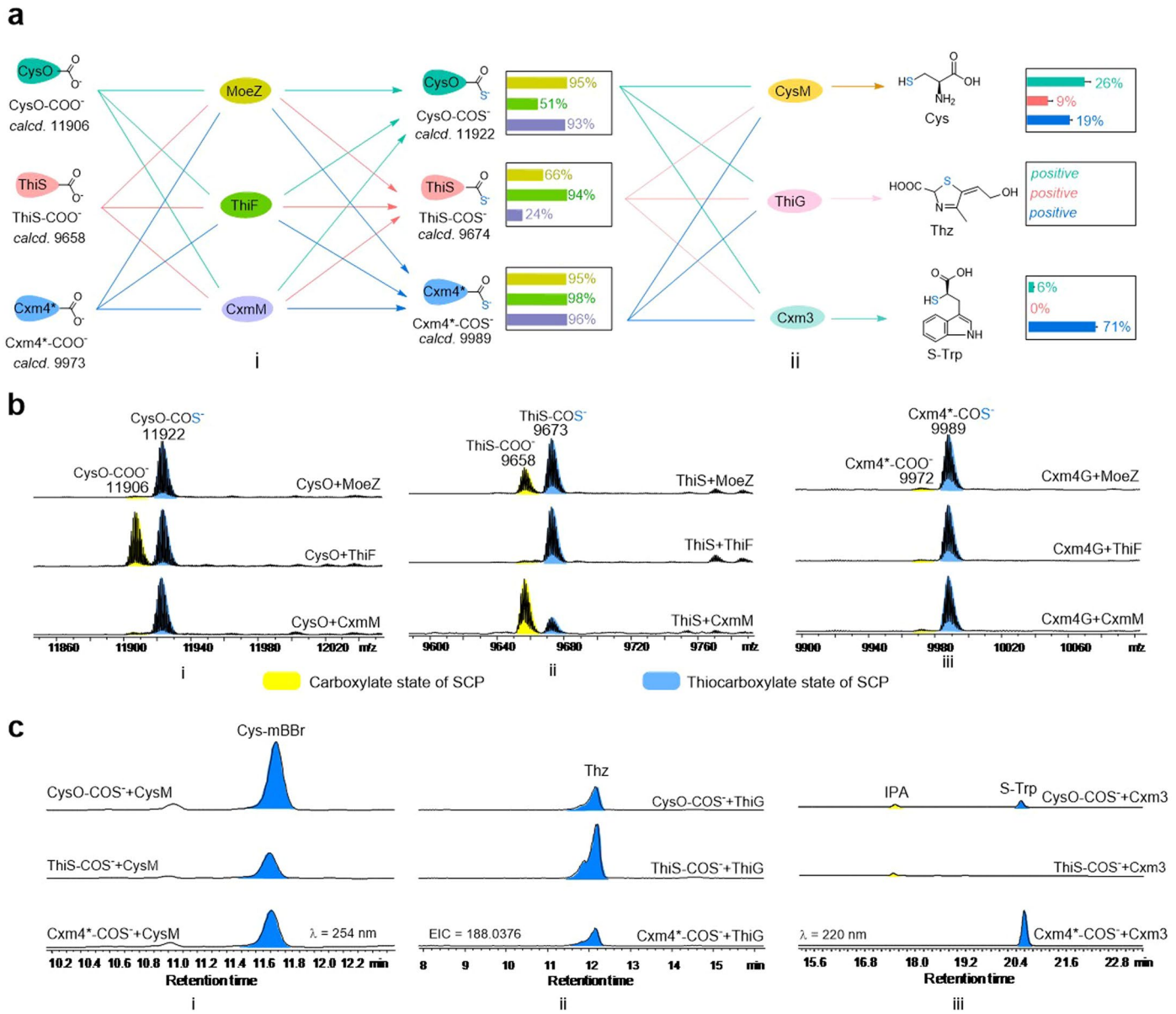

Extended Data Fig. 7 | Recombination in the SCP-based sulfur incorporation systems. a, Recombination network of SCPs against different activating enzymes MoeZ, ThiF, and CxmM (i) and sulfurtransferases CysM, ThiG, and Cxm3 (ii). The *left* boxed histograms show the conversion ratios of SCPs (i). The *right* boxed histograms show the yields of organosulfur products in one-pot reactions (ii) of the three recombined pathways (the yield of Thz was not determined due to unavailability of authentic standard. 'Positive' indicates the product was detectable by LC-MS). The colour of each column represents the corresponding same coloured activating enzyme (i) or SCP (ii) supported reaction. **b**, Deconvoluted HRESI-MS analyses of the selenylation efficiency of CysO (i), ThiS (ii) and Cxm4* (iii) by different activating enzymes. **c**, HPLC (i and iii) and HPLC-MS (ii) analysis of the sulfur-transfer reactions of Cys (i), Thz (ii) and S-Trp (iii) by different sulfurtransferases.

nature portfolio

Corresponding author(s): Shengying Li

Last updated by author(s): Dec 5, 2023

Reporting Summary

Nature Portfolio wishes to improve the reproducibility of the work that we publish. This form provides structure for consistency and transparency in reporting. For further information on Nature Portfolio policies, see our Editorial Policies and the Editorial Policy Checklist.

Statistics

For all statistical analyses, confirm that the following items are present in the figure legend, table legend, main text, or Methods section.

n/a	Confirmed
☐	☒ The exact sample size (*n*) for each experimental group/condition, given as a discrete number and unit of measurement
☐	☒ A statement on whether measurements were taken from distinct samples or whether the same sample was measured repeatedly
☒	☐ The statistical test(s) used AND whether they are one- or two-sided *Only common tests should be described solely by name; describe more complex techniques in the Methods section.*
☒	☐ A description of all covariates tested
☒	☐ A description of any assumptions or corrections, such as tests of normality and adjustment for multiple comparisons
☐	☒ A full description of the statistical parameters including central tendency (e.g. means) or other basic estimates (e.g. regression coefficient) AND variation (e.g. standard deviation) or associated estimates of uncertainty (e.g. confidence intervals)
☒	☐ For null hypothesis testing, the test statistic (e.g. *F*, *t*, *r*) with confidence intervals, effect sizes, degrees of freedom and *P* value noted *Give P values as exact values whenever suitable.*
☒	☐ For Bayesian analysis, information on the choice of priors and Markov chain Monte Carlo settings
☒	☐ For hierarchical and complex designs, identification of the appropriate level for tests and full reporting of outcomes
☒	☐ Estimates of effect sizes (e.g. Cohen's *d*, Pearson's *r*), indicating how they were calculated

Our web collection on statistics for biologists contains articles on many of the points above.

Software and code

Policy information about availability of computer code

Data collection	No custom code was used NMR data were collected by Bruker Topspin 4.1.4 HPLC-MS data were collected by Bruker Compass for otofSeries 1.7 HPLC data were collected by Agilent Open Lab 3.2.0
Data analysis	No custom code was used Bruke DataAnalysis 4.2 for HPLC-MS data analysis MestReNova 14.1 for NMR data analysis Agilent Open Lab 3.2.0 for HPLC data analysis

For manuscripts utilizing custom algorithms or software that are central to the research but not yet described in published literature, software must be made available to editors and reviewers. We strongly encourage code deposition in a community repository (e.g. GitHub). See the Nature Portfolio guidelines for submitting code & software for further information.

Data

Policy information about availability of data

All manuscripts must include a data availability statement. This statement should provide the following information, where applicable:

- Accession codes, unique identifiers, or web links for publicly available datasets
- A description of any restrictions on data availability
- For clinical datasets or third party data, please ensure that the statement adheres to our policy

Experimental data supporting the conclusions of this study are available within the article and its Supplementary information. Protein sequences were retrieved from the NCBI protein database (https://www.ncbi.nlm.nih.gov/protein/) with the accession numbers in Supplementary Table 1.

Human research participants

Policy information about studies involving human research participants and Sex and Gender in Research.

Reporting on sex and gender	n/a
Population characteristics	n/a
Recruitment	n/a
Ethics oversight	n/a

Note that full information on the approval of the study protocol must also be provided in the manuscript.

Field-specific reporting

Please select the one below that is the best fit for your research. If you are not sure, read the appropriate sections before making your selection.

☒ Life sciences ☐ Behavioural & social sciences ☐ Ecological, evolutionary & environmental sciences

For a reference copy of the document with all sections, see nature.com/documents/nr-reporting-summary-flat.pdf

Life sciences study design

All studies must disclose on these points even when the disclosure is negative.

Sample size	Following common practice in the field of enzymatic catalysis, all the bioassays were independently performed in triplicate.
Data exclusions	No data were excluded.
Replication	All bioassays were repeated at least three independent times. All results were reliably reproduced.
Randomization	To determine the enzymatic activities of the SCP-based systems with regard to selenium incorporation, the reactions with selenium sources were allocated into experimental groups, and the similar reactions with sulfur sources were set as positive control experiments, and also, the reactions with boling-inactivated SCPs were set as negative control reactions. The selection and the order for reproduction of the reactions as well as sample analyses were random.
Blinding	Blinding was not relevant for this study, because all reactions and samples were labeled, randomly tested and analyzed.

Reporting for specific materials, systems and methods

We require information from authors about some types of materials, experimental systems and methods used in many studies. Here, indicate whether each material, system or method listed is relevant to your study. If you are not sure if a list item applies to your research, read the appropriate section before selecting a response.

Materials & experimental systems

n/a	Involved in the study
☒	☐ Antibodies
☒	☐ Eukaryotic cell lines
☒	☐ Palaeontology and archaeology
☒	☐ Animals and other organisms
☒	☐ Clinical data
☒	☐ Dual use research of concern

Methods

n/a	Involved in the study
☒	☐ ChIP-seq
☒	☐ Flow cytometry
☒	☐ MRI-based neuroimaging